

Probing the underground at the Badenian type locality: geology and sedimentology of the Baden-Sooss section (Middle Miocene, Vienna Basin, Austria)

MICHAEL WAGREICH¹, PETER PERVESLER², MAKSUDA KHATUN³, INGE WIMMER-FREY⁴
and ROBERT SCHOLGER⁵

¹Department of Geodynamics and Sedimentology, Center for Earth Sciences, University of Vienna, Althanstrasse 14, 1090 Vienna, Austria; michael.wagreich@univie.ac.at

²Department of Paleontology, University of Vienna, Althanstrasse 14, 1090 Vienna, Austria; peter.pervesler@univie.ac.at
³27 Tarington Way NE, Calgary, AB, T3J 4N1, Canada; maksuda.khatun@gmail.com

⁴Geological Survey of Austria, Neulinggasse 38, 1030 Vienna, Austria; i.wimmer-frey@geologie.ac.at

⁵Chair of Geophysics, Paleomagnetic Laboratory Gams, MU Leoben, Austria; robert.scholger@mu-leoben.at

(Manuscript received December 13, 2007; accepted in revised form June 12, 2008)

Abstract: A 102 m long core of fine-grained sediments of the Vienna Basin (Baden Group, “Badener Tegel”) was drilled at the Badenian type locality outcrop in Baden-Sooss. An Early Badenian age (regional Upper Lagenidae Foraminiferal Zone) is indicated by biostratigraphy. The core comprises mainly bioturbated, medium to dark grey marls and shales with a slightly higher degree of tectonic deformation in the upper part of the core. XRD indicates mainly quartz, muscovite/illite, chlorite, feldspar, calcite and minor dolomite as constituents. Carbonate contents vary between 10 % and 35 % and organic carbon between 0.32 % and 0.78 %. Rare intercalations include sand layers with shell debris, a conglomerate and a smectitic tuff layer. Mean grain size ranges from 4 to 8 µm. Cyclic sedimentation was identified by rhythmic variations in carbonate and organic carbon contents and magnetic susceptibility. Rock Eval pyrolysis indicates mainly type III kerogen from terrestrial higher plant material and minor marine input. The depositional environment can be characterized as offshore, below the fair-weather wave base but within the storm-wave base. The sediments are hemipelagites, transported by pelagic suspension, that is a mixture of pelagic biogenic carbonate, mainly calcareous nannofossils and foraminiferal tests, and terrigenous clay and silt. The positive correlation of carbonate to organic carbon indicates a dilution controlled siliciclastic deposition with varying siliciclastic input. Except for minor primary laminated intervals, oxygenated bottom water conditions are reconstructed from the presence of various trace fossils and ichnofabrics from the *Zoophycos* ichnofacies in the deeper part with a transition to the distal *Cruziana* ichnofacies towards the top of the core.

Key words: Miocene, Badenian, Vienna Basin, sedimentology, geochemistry, clay mineralogy, hemipelagite.

Introduction

The Neogene Vienna Basin is situated at the junction of the Eastern Alps and the Western Carpathians, within the territories of Austria, the Slovak and the Czech Republics (e.g. Wesely 1988; see Fig. 1). The basin has been a classical area of geological and paleontological investigations of Miocene strata since the 19th century (e.g. Keferstein 1828; d’Orbigny 1846; Reuss 1848; Hörnes 1856). Numerous studies have been applied to the deposits and their paleontological content, also triggered by significant hydrocarbon findings during the 20th century (Hamilton et al. 2000). However, the lack of natural outcrops restricts detailed sedimentological and paleontological analysis of Vienna Basin strata to a decreasing number of active clay pits and quarries.

The fine-grained sediments of the “Badener Tegel” of Middle Miocene age constitute a classical lithofacies type of the Vienna Basin (Keferstein 1828) and yield a wealth of macro- and microfossils (e.g. d’Orbigny 1846). Modern sedimentological investigations on the “Badener Tegel” are largely missing because of the lack of suitable outcrops. Supported by the Austrian Science Fund FWF-Project P13743-BIO “Tem-

poral and spatial changes of microfossil associations and ichnofacies in the Austrian marine Miocene” a scientific core has been drilled in January to February 2002, near the western margin of the southern Vienna Basin (Fig. 1). The drill hole reached a depth of 102 meters and was cored throughout. The aim of this scientific borehole Baden-Sooss was a detailed investigation of freshly cored Badenian sediments at the type locality of the Badenian, the former clay pit Baden-Sooss (compare Papp & Steininger 1978; Rögl et al. 2008). Multidisciplinary studies were applied for evaluating biostratigraphy, paleoecology, paleoichnology, sedimentology, geochemistry, magnetostratigraphy and magnetic climate proxies such as magnetic susceptibility (Hohenegger et al. 2008). This paper presents data on the geology, sedimentology and geochemistry from samples of the core of the scientific borehole Baden-Sooss.

Geological setting

The scientific borehole Baden-Sooss (Fig. 1) penetrated a succession of Badenian (Langhian, Middle Miocene; Fig. 2)

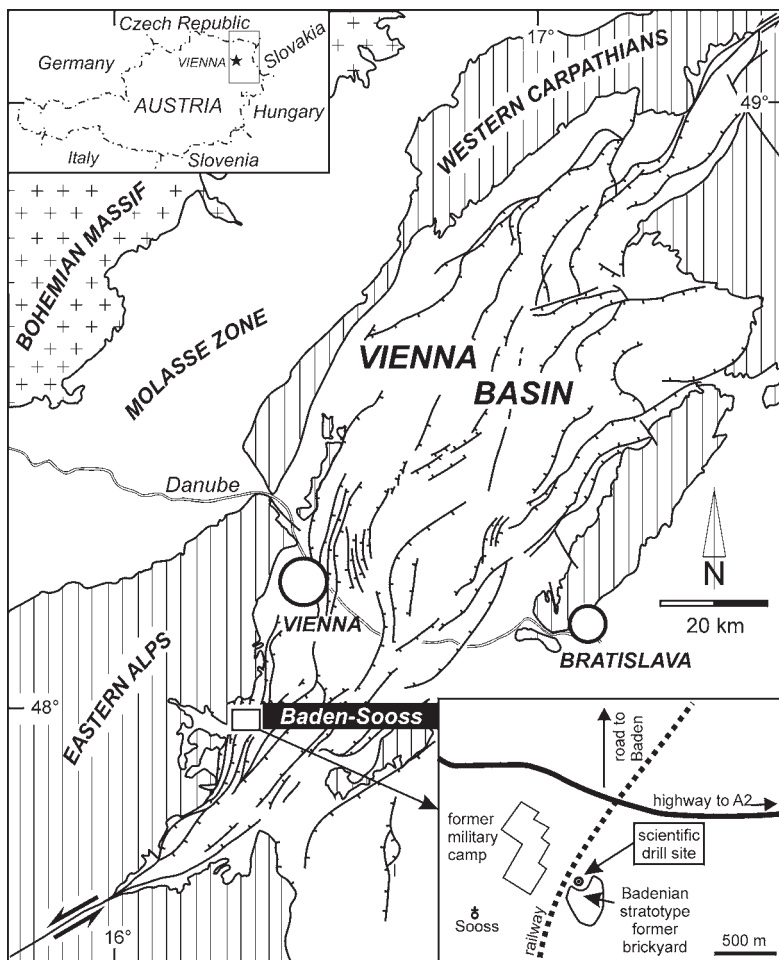


Fig. 1. Tectonic sketch map of the Vienna Basin (modified from Decker 1996, and Wagreich & Schmid 2002; Neogene = white) at the junction of the Eastern Alps and the Western Carpathians (hatched areas) and location of the studied borehole Baden-Sooss in the surroundings of Sooss and Baden (map modified from Wessely in Rögl et al. 2008).

fine-grained deposits, starting from the type section of the Badenian stage, the old brickyard Baden-Sooss to the south of the town of Baden (geographic coordinates WGS84: E 016° 13' 44", N 47° 59' 24") (Papp et al. 1978; see also discussion by Rögl et al. 2008). Thus, the borehole explored the subsurface of the stratotype section which was defined and described by Papp & Steininger (1978). The borehole site was situated some tens of meters to the north of the margin of the former clay pit (for a detailed geological map of the area including the drill site see Rögl et al. 2008: fig. 2). As outcrops in this pit are now limited due to extensive filling by waste material and restricted to a partly covered old pit face preserved as a natural monument, and hidden faults may be present between the drill site and the outcrops, the core section could not be directly correlated into the stratotype outcrop. However, from the geological data and the dipping of the beds, it becomes clear, that the core strata represent more or less the direct substrate of the stratotype, although some meters of strata may be missing due to the above mentioned reasons. Basinward, according to borehole data given by Brix

& Plöchinger (1988), Badenian fine-grained strata thicken considerably across synsedimentary normal faults.

The Vienna Basin is a rhomb-shaped SSW-NNE oriented basin of about 200 km long and 55 km wide. The basin forms a thin-skinned Miocene pull-apart basin (Royden 1985) and constitutes a marginal basin of the Central Paratethys (for paleogeographic overview see, e.g. Rögl 1998, 1999; Hámor 2001; Kvaček et al. 2006; Strauss et al. 2006). The basin formed due to left-lateral transtension and strike-slip between the Alps and the Carpathians (e.g. Ratschbacher et al. 1991; Decker 1996; Hamilton et al. 2000; Hinsch et al. 2005).

Stratigraphy

The stratigraphy of the Vienna Basin has been a subject of studies since the nineteenth century. Paleontological monographs (e.g. d'Orbigny 1846; Hörnes 1856, 1870; Karrer 1867) were followed by detailed stratigraphic analysis (see also Rögl et al. 2008). Grill (1941, 1943) established zonation by foraminifera, followed by significant stratigraphic works such as those by Papp (1951, 1953) and Steininger & Papp (1979).

Based on these classical works and more recent publications (e.g. Hamilton et al. 2000; Kováč et al. 2004; Strauss et al. 2006) the evolution of the Vienna Basin started during the Early Miocene (Eggenburgian-Ottangian-Karpatian of Central Paratethys stages) with the development of a partly non-marine piggy-back basin on top of Alpine thrusts to the northeast of Vienna (Decker 1996). Sinistral transtension during the Early/Middle Miocene led to the formation of small-scale, rapidly subsiding lows and relatively stable highs during the Badenian. This first phase of tectonically controlled subsidence is considered to be a result of the initial pull-apart rifting stage (Lankreijer et al. 1995). Depocenters of the basin shifted towards the south, being filled by a large delta that developed in its southern part. In the Early Badenian, NE-SW oriented faulting occurred on the western margin of the basin. Marine transgression started during this time and also reached the southern part of the basin. Up to 3000 m thick successions of fully marine Badenian marls characterize the central parts of the basin, whereas delta sands and limestones were deposited on the basin margins or at shallow depths during this time (Sauer et al. 1992; Weissenböck 1996; Seifert 1996). During Sarmatian and Pannonian times, salinity oscillated and finally decreased, leading to limnic-fluvial deposits (Harzhauser & Piller 2005a,b, 2007).

Strauss et al. (2006) divided the Neogene sediments in the southern Vienna Basin into five Middle and Upper Miocene 3rd-order depositional sequences, the Badenian comprising three of these depositional sequences starting with coarse clas-

tics and carbonates at the base. The middle part of the Badenian represents a thin lowstand with eroded carbonate material at the base followed by sand and silt deposition. The upper part of the Badenian is characterized by sand and clay in the lower part and carbonates in the upper part (Strauss et al. 2006).

In the central and southern Vienna Basin the Badenian sediments are divided into proximal deltaic clastics and a distal basinal facies, which is characterized by sandy marls and clays. On the eastern border of the Vienna Basin and in other partly protected marginal areas, corallinacean limestones ("Leithakalk", e.g. Strauss et al. 2006; Harzhauser & Piller 2007) were deposited during periods of sea-level highstand in the Badenian.

Widespread fine-grained grey Badenian "basinal" deposits of the offshore, deeper parts of the basin comprise mixtures of clay and silt, containing significant amounts of illite, chlorite and some smectite as reported by Wagner & Czurda (1991). The first descriptions of these fine-grained sediments date back to Keferstein (1828) who recognized grey-bluish clays locally named "Tegel" around the town of Baden. Later on, Papp & Steininger (1978) described the Badenian sediments in the framework of the stratotype definition of the Badenian as greyish-blue, plastic clay with a yellowish weathering in the uppermost portion, including minor sand lenses with molluscs. The clays appear massive to crudely bedded in the outcrop and a total of 14 meters of section was documented by Papp & Steininger (1978: fig. 30; see also Rögl et al. 2008).

The lithostratigraphic division of these sediments in the Austrian part of the basin is still under debate. During the 19th and first half of the 20th century only the term "mariner Tegel von Baden" or "Badener Tegel" was in use. In the revision of Austrian Neogene stratigraphic nomenclature for the marine Middle Miocene sediments of the Vienna Basin by Papp et al. (1968), the stratigraphic term "Badener Serie" as a formation (Baden Formation) has been introduced but a clear differentiation between litho-, bio-, and chronostratigraphy was not provided. The recent lithostratigraphic chart of Austria (Piller et al. 2004) places the "Badener Tegel" into the Baden Group, which can be subdivided into the Jakobov Formation and the Lanžhot Formation in the Slovak part of the basin (Kováč et al. 2004). The lower part of the Badenian including the Baden-Sooss core may thus be correlated to the Lanžhot Formation.

Biostratigraphic investigations on foraminifera (mainly lower part of the local Upper Lagenidae Zone, see Hohenegger et al. 2008a) and calcareous nannoplankton (standard Zone NN5, see Čorić & Hohenegger 2008) indicate an Early Badenian (Langhian) age (Fig. 2). Hohenegger et al. (2008a) dated the core by cyclostratigraphy and orbital tuning to -14.379 ± 1 and $-14.142 \text{ Myr} \pm 9 \text{ kyr}$.

The succession at Baden-Sooss was correlated to the lowermost 3rd-order sequence of the Badenian in the Vienna Basin, sequence VB5 of Kováč et al. (2004) or Ba1 of Strauss et al. (2006). Transgressive conglomerates form the base of this sequence. The top of this sea-level cycle is associated with a major sea-level drop throughout the Vienna Basin (e.g. Weissenböck 1996), which was correlated with a worldwide drop in sea level from 14.2 to 13.8 Ma including the

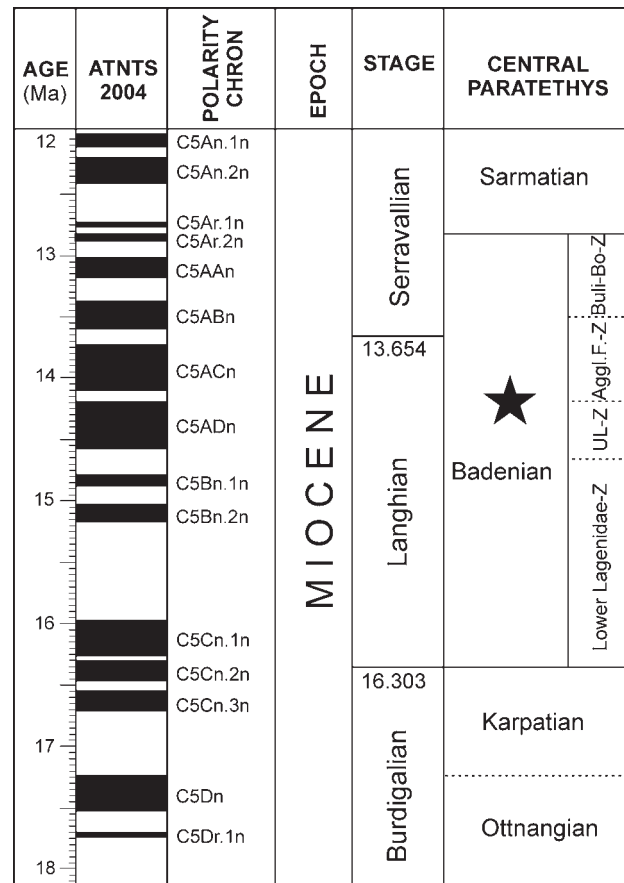


Fig. 2. Lower to Middle Miocene stratigraphic chart based on the time scale of Lourens et al. (2004); the black star denotes approximate stratigraphic position of the Baden-Sooss core based on cyclostratigraphy according to Hohenegger et al. (2008a). Abbreviations of local zones: UL-Z = Upper Lagenidae Zone, Aggl.F.-Z = Zone of agglutinated foraminifera, Buli-Bo-Z = *Bulimina-Bolivina* Zone.



Fig. 3. Photograph of drilling equipment (February 2002) at Baden-Sooss and position near northern margin of the former clay pit.

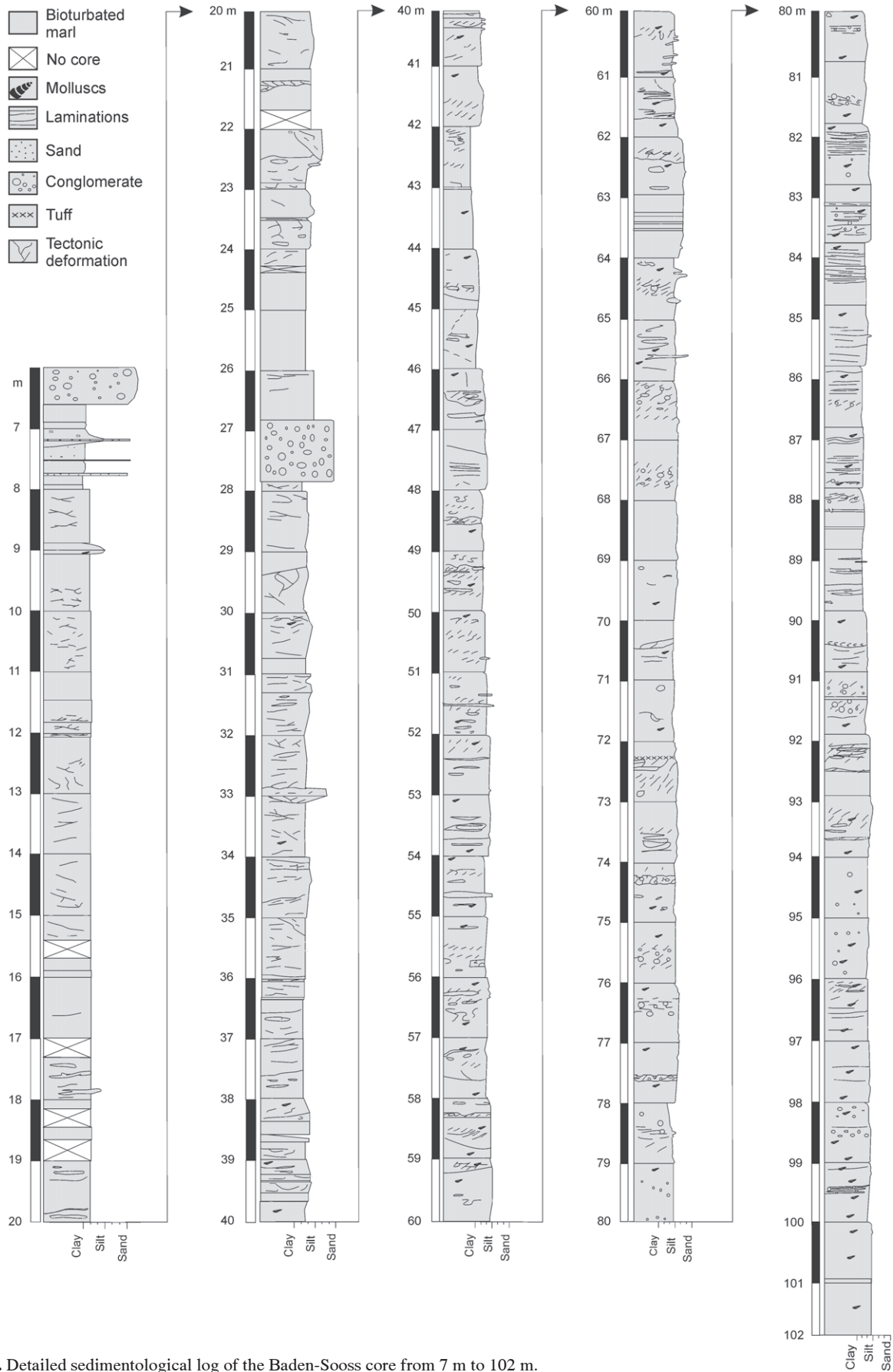


Fig. 4. Detailed sedimentological log of the Baden-Sooss core from 7 m to 102 m.

Lan2/Ser1 sequence boundary of Hardenbol et al. (1998; see Strauss et al. 2006 and Harzhauser & Piller 2007). However, the correlation of these regional sea-level cycles to the global sea-level curve still remains debateable.

Material and methods

Drilling the uppermost 8 meters delivered gravel and loose pebbles of probable Quaternary age. Cores with a diameter of 15 cm were taken continuously from 8 to 102 m. After splitting the core vertically and smoothing the cross-section a thorough digital documentation was performed by whole core scanning and digital photography (see Appendix 1A–I). These image series were also used for the ichnological analysis. A sedimentological log of the core was documented by visual analysis, forming the base for further investigations and sampling (Fig. 4).

Half of the split core was preserved and stored at the Department of Paleontology, University of Vienna. The second half was used as a source of samples for sedimentology, geochemistry, microfossils, nannofossils and paleomagnetic analysis. Trace fossils were detected from 8 to 102 meters core depth. Additional cuts were made horizontally to the bedding.

For representative grain size analysis, wet sieving and X-ray sedigraph techniques have been applied. Five representative samples were taken from the Baden-Sooss core at depths of 20–20.10 m, 40.35–40.45 m, 60.05–60.15 m, 80.20–80.30 m, 100.15–100.25 m. The samples were crushed and dried. Each sample was prepared by adding distilled water containing 0.5% sodium hexametaphosphate, disaggregated for 24 hrs and analysed. The Sedigraph 5000 ET produced measurements for sediments of a grain size smaller than 70 μm . Coarser fractions were sieved using a sieve at $>63 \mu\text{m}$ prior to the sedigraph measurements. The relative proportions of the sand, silt and clay fractions were determined. Various statistical parameters for grain size interpretation were calculated.

Overview carbonate and organic carbon analyses were performed on a set of 22 core samples from 5 m intervals. Detailed carbonate and organic carbon analyses were measured on 310 samples collected from 40 to 102 m depth (sample interval 20 cm). Calcium carbonate was analysed using the carbonate bomb technique of Müller & Gastner (1971). Powdered samples of 1 g were dissolved in 15% hydrochloric acid. Carbonate dissolved and the pressure of the evolved CO_2 gas were measured and converted to percentages of CaCO_3 using calibration curves. Each sample was measured at least two times. The error of the result is $\pm 0.5\%$. For analysis of organic carbon contents, the same sample sets were dried at room temperature prior to grinding with a powder grinding mill. The standard procedure involves heating the weighted dry sediment samples to 550 °C and measuring the combustion product CO_2 gases by gas chromatography using a LECO RC-412 device.

The same samples analysed for organic carbon were used for Rock Eval pyrolysis (laboratories of Baseline Resolution Inc. Shenandoah, Texas). The ground rock samples were heated in an inert gas atmosphere at a programmed rate while amounts of volatile hydrocarbons (S1), and of hydrocarbons

(S2) and CO_2 (S3) released from the kerogen were measured. The amount of hydrocarbons (mgHC/g rock) released from kerogen during heating was normalized against TOC, to give the Hydrogen Index (HI; Espitaliè et al. 1977). The temperature at which the maximum release of hydrocarbons occurred (T_{max}) was also recorded as a maturation indicator.

For a geochemistry scan by routine XRF analysis, the overview samples with a sample distance of 5 m were used. The same sample set was used for mineralogy and clay mineralogy analysis by XRD. The bulk and clay mineralogy of 20 core samples at a 5 m interval was determined by XRD. For bulk mineral analysis the dried samples were ground and loaded into a sample holder as a randomly oriented powder. Diffraction data were collected with a Philips X'Pert Multi Purpose Diffractometer (goniometer PW 3050), Cu-K α radiation (40 kV, 40 mA), automatic divergence slit, 0.30 mm receiving slit, step scan (step size 0.02° 2 Θ 1 second per step). The samples were run from 2–65° 2 Θ . The semiquantitative mineralogical composition was obtained using a computer program (Paktunc 1998) incorporating information from bulk chemical analyses.

For clay mineral analysis the samples were treated with H_2O_2 in order to remove organic matter and with ultrasound for further disaggregation. The $<2 \mu\text{m}$ fractions were separated by centrifugation. The clay fractions were saturated with 1 N KCl-solutions and 1 N MgCl_2 -solutions by shaking 24 h and afterwards washed in distilled water. Oriented preparations of the $<2 \mu\text{m}$ fractions were achieved by suction of 25 mg clay in suspension on a porous ceramic plate and drying at room temperature. Oriented XRD mounts were then analysed in the air dried, ethylene glycol, dimethylsulfoxide, glycerol, 300° and 550 °C treated states. The clay samples were run from 2–50° 2 Θ with the same step and counting time as the bulk samples. The identification of clay minerals was carried out according to Moore & Reynolds (1997).

Various rock magnetic investigations were performed on the core (for details see Selge 2005). Here, only magnetic susceptibility measurements are reported and evaluated (see also Hohenegger et al. 2008a). Laboratory measurements were performed on standard paleomagnetic sample cubes for unconsolidated rocks (sampling interval between 25 and 70 cm). All laboratory magnetic measurements were carried out in the Paleomagnetic Laboratory Gams of the University of Leoben (Austria). The measurements included volume- and mass-specific susceptibility and anisotropy of magnetic susceptibility (AMS). Magnetic volume susceptibility was furthermore measured on the full length of the drill core with an Exploranium KT9 susceptibility-meter. The measurements were performed at 5 cm point distances to produce a continuous susceptibility log of the core.

Lithology and log

In general the Baden-Sooss core displays a higher degree of tectonic deformation in the upper 40 meters (Fig. 4 and Appendix 1A–C). This penetrative deformation is recognizable by the presence of some small-scale fault planes, which show vertical throws of a few mm to cm (Appendix 1A–C).

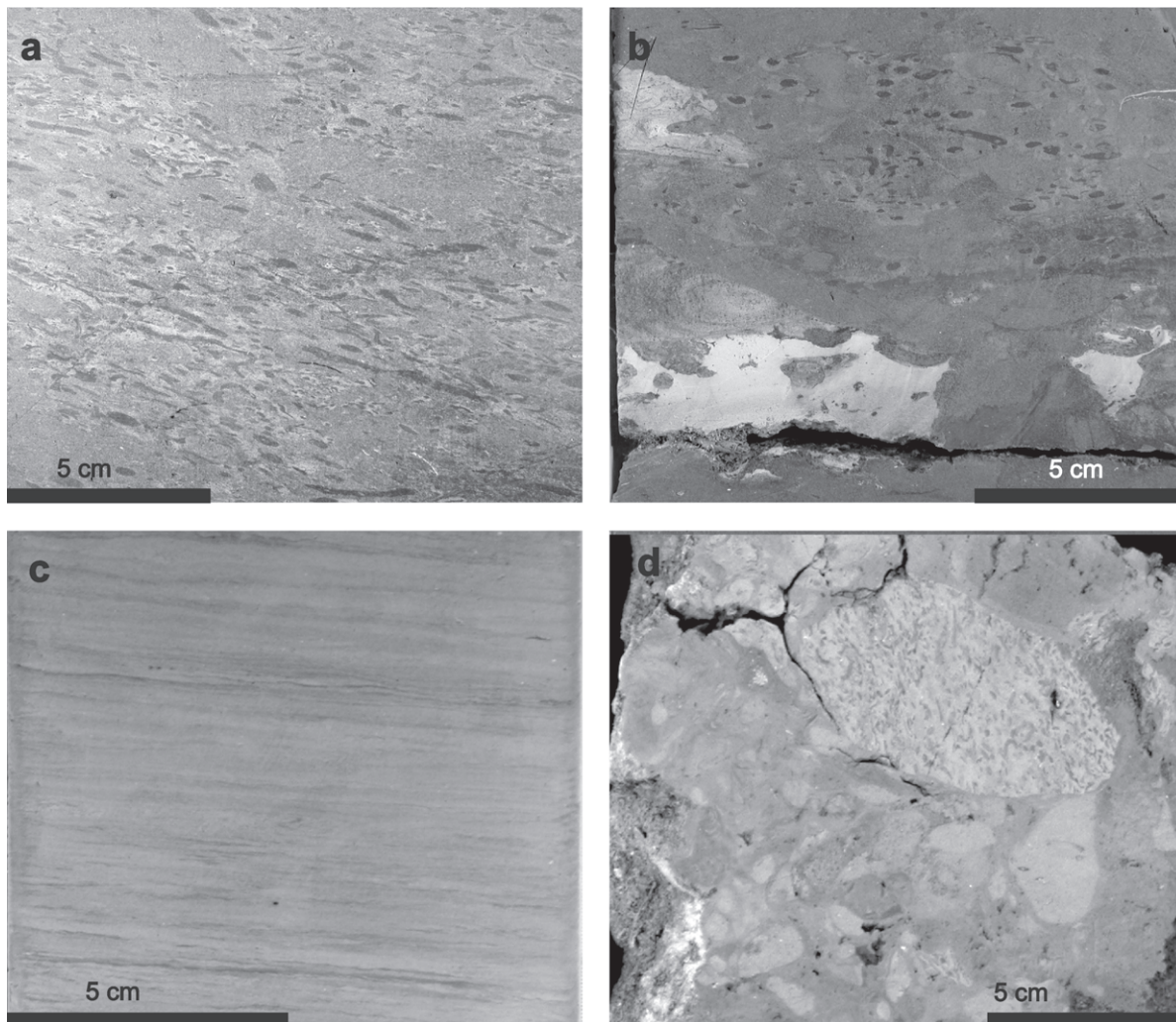


Fig. 5. Typical facies of the Baden-Sooss core: **a** — bioturbated marl facies, mainly *Phycosiphon* (core 17.0 m); **b** — bioturbated tuff layer (core 72.4 m); **c** — laminated facies (core 84.5 m); **d** — intraformational conglomerate (core 22.0 m).

Fault planes often appear darker due to concentration of clay minerals on the surfaces. These more intensely deformed rocks can thus be classified as protocataclasites. Despite small displacements the lithology itself is not strongly influenced by these tectonic deformations. Below 40–45 m, the fault planes die out completely. Tectonic deformation is interpreted as a result of a young set of faults connected to a major fault in the nearby stratotype Baden-Sooss which displaces Badenian against Sarmatian strata (Papp & Steininger 1978).

On the basis of visual investigations four general lithofacies have been recognized in the Neogene part of the core below 8 m (Fig. 5). Fine-grained marls and clays (“Badener Tegel”) constitute more than 95 % of the core (Fig. 5a). Most of the core marls are bioturbated, only a few intervals of laminated marls and clays occur (Fig. 5c; see also Appendix 1H). Sand layers are minor (<5 % of the total core log) and often strongly bioturbated; rare mollusc shells are present in such coarser layers (Appendix 1A). An intraformational conglomerate occurs at around 27 m (Fig. 5d; see also Appendix 1B), and a light grey 5 cm tuff layer is present at 72.5 m (Fig. 5b). No regular variations in lithofacies or general trends along the

core length have been recognized, except that sand layers are slightly more common in the upper part of the core.

Sedimentology

Within the marl lithofacies, bioturbation is extremely common and dense, obliterating most primary sedimentary structures except for a few short intervals in the lower part of the core around 80 to 85 m (Fig. 5c). There, primary light-dark horizontal laminations of lower flow regime origin are (partly) preserved, although thin section analysis indicates the presence of some micro-burrows also in these laminated layers.

Due to bioturbation (see Appendix 1), detailed investigations on ichnofossils and ichnofabric analysis were essential for the interpretation of the depositional environment and the recognition of changes in ecological parameters like oxygenation, nutrients, stability of the environment and the substrate (see Pervesler et al. 2008). Trace fossils from the ichnogenera *Asterosoma*, *Chondrites*, *Nereites*, *Ophiomorpha*, *Phycosiphon*, *Scolicia*, *Siphonichnus*, *Teichichnus*, *Thalassinoides*,

Trichichnus and *Zoophycos* were distinguished in cross-section. *Phycosiphon* and *Nereites* are the most common trace fossils observed in most horizons. *Asterosoma*, *Trichichnus* and *Zoophycos* are important elements of the deeper parts in the core; *Thalassinoides* filled with slightly coarser sediment occurs in the higher parts from 65 to 8 meters. The co-occurrence of certain trace fossils made clustering into several ichnofabric types supposable (Pervesler et al. 2008).

Grain size analyses

The analysed grain size of the marls from the Baden-Sooss core did not indicate any significant trend from bottom to top of the core (Fig. 6a). The sediment is dominated by particles smaller than 2 μm (53 %) and particles ranging from

2–44.42 μm (45 %), which corresponds to the clay and fine/medium-sized silt fractions. Very small portions (1.5 %) of the sediments range into the fine sand size fraction. The ternary diagram plot of the different fractions of the sediments indicates mainly silty clay (Fig. 6b). They basically bear a pelitic texture and the size trends (Table 1) are mainly bimodal except in the sample from 40 m (polymodal) and 80 m (trimodal). The sample from 80 m represents the lower part of the core which comprises light-dark laminated intercalations. The mean grain size falls into fine silt and clays with median values (Folk & Ward 1957) from 4 to 6 μm . The sample at 40 m also contains a significant proportion (17 %) of coarse silt. The sorting is rather poor for all the samples (Table 1) and can be classified as poorly sorted to very poorly sorted according to the classification of Folk & Ward (1957). Skewness is sym-

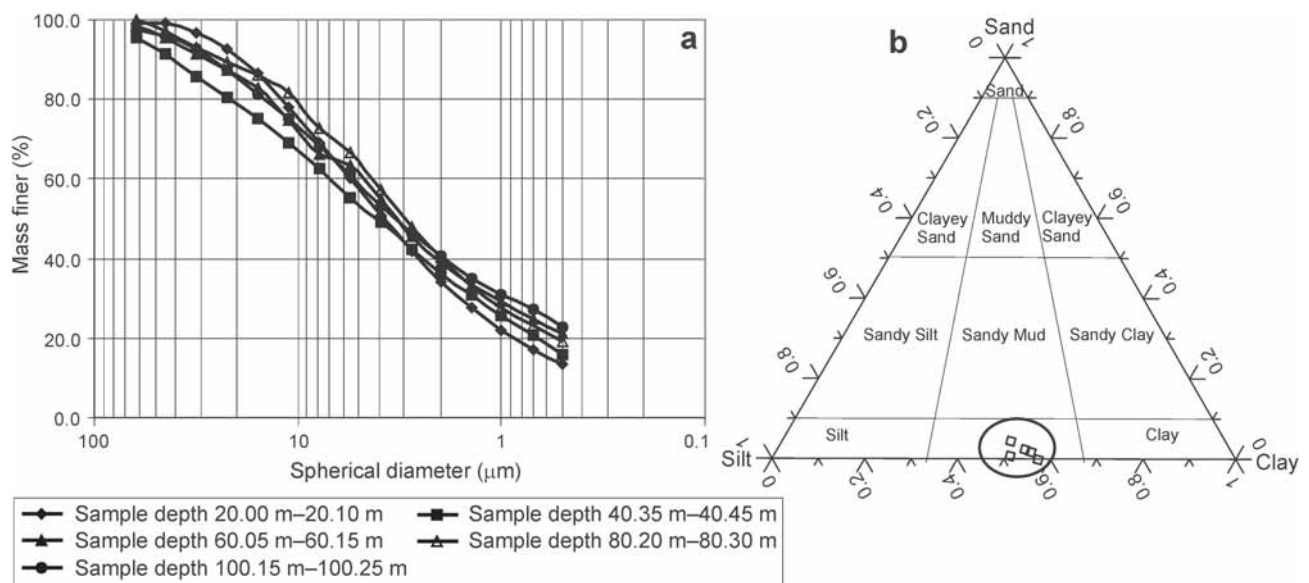


Fig. 6. (a) Grain size cumulative frequency curves and (b) position of samples in a ternary classification diagram Sand-Silt-Clay.

Table 1: Grain size characteristics of the Baden-Sooss core, parameters according to method of moments (e.g. Blott & Pye 2001) and Folk & Ward (1957).

	Sample meter	20 m	40 m	60 m	80 m	100 m
	SAMPLE TYPE	Bimodal, poorly sorted	Polymodal, very poorly sorted	Bimodal, poorly sorted	Trimodal, poorly sorted	Bimodal, poorly sorted
METHOD OF MOMENTS Arithmetic (μm)	Mean	8.065	11.35	10.24	9.656	9.765
	Sorting	8.669	14.14	12.57	12.77	11.44
	Skewness	1.947	1.634	1.925	2.106	1.849
	Kurtosis	7.338	4.789	6.252	6.756	6.260
FOLK AND WARD METHOD (μm)	Mean	4.690	6.386	5.413	4.559	5.623
	Sorting	3.175	4.559	3.722	3.516	3.754
	Skewness	-0.043	0.027	0.093	0.102	-0.004
	Kurtosis	0.896	0.841	0.929	0.986	0.893
FOLK AND WARD METHOD (ϕ)	Mean	7.736	7.291	7.529	7.777	7.474
	Sorting	1.667	2.189	1.896	1.814	1.908
	Skewness	0.043	-0.027	-0.093	-0.102	0.004
	Kurtosis	0.896	0.841	0.929	0.986	0.893
FOLK AND WARD METHOD (Description)	Mean	Fine silt	Fine silt	Fine silt	Fine silt	Fine silt
	Sorting	Poorly sorted	Very poorly sorted	Poorly sorted	Poorly sorted	Poorly sorted
	Skewness	Symmetrical	Symmetrical	Symmetrical	Coarse skewed	Symmetrical
	Kurtosis	Platykurtic	Platykurtic	Mesokurtic	Mesokurtic	Platykurtic

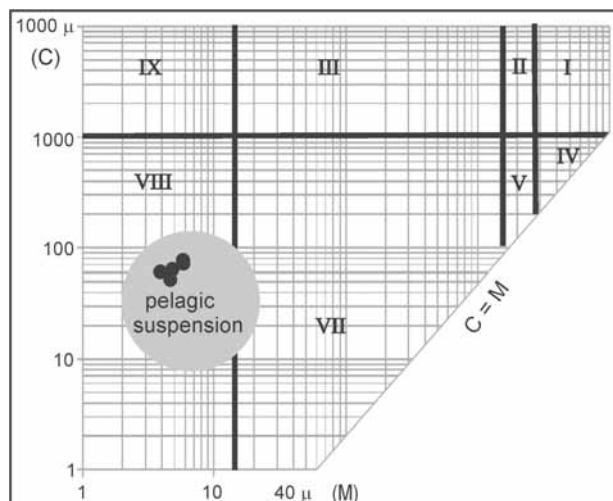


Fig. 7. Position of samples in Passega's (1964) CM-diagram.

metrical except at 80 m which shows a coarse skewness. Kurtosis is platykurtic or mesokurtic. The samples plot into the field of pelagic suspension transport (VIII) according to the CM-diagram (Fig. 7) of Passega (1964).

Carbonate contents

In the 22 overview samples the carbonate values vary from 11 % to 25 % of the total weight (Fig. 8a). Two large cycles are visible even in this coarse sample resolution (see Hohenegger et al. 2008a). Carbonate values increase from the bottom of the section up to a maximum value of 25 % at 50 m, then values decrease again from 40 m up to the top. The high resolution analysis (20 cm sample distance from 40–102 m core) illustrates that the percentage of carbonate content varies from 10 % to 35 % (Fig. 8b). In average, the content is 18 % within this 60 m thick succession. A clear cyclicity including 6 cycles within the lower part of the section can be recognized by moving average conversion (Fig. 8c).

Organic carbon contents

Organic carbon varies from 0.32 % to 0.78 % of the total weight along with fluctuations of carbonate contents (Fig. 9a,b). The percentage starts with the highest values of around 0.78 % at 95 m depth of the section, and then oscillates between values below and above 0.60 % (Fig. 9a). A general trend from slightly higher to lower values from bottom to top of the section is recognized. The fluctuation of the distribution of organic carbon throughout the section (Fig. 9b,c) indicates a cyclic pattern (see Hohenegger et al. 2008a). No distinct organic carbon peak is associated with the laminated part of the core at around 84.5 m.

C_{org} - $CaCO_3$ curves

The carbonate ($CaCO_3$) and organic carbon (C_{org}) contents of the Baden-Sooss core were plotted in C_{org} - $CaCO_3$ diagrams to evaluate the basic sediment flux and depositional

model in the pelagic/hemipelagic carbonate-siliciclastic-organic carbon three-component system (see Ricken 1991, 1993). The diagram (Fig. 10) shows a linear positive relation between C_{org} and $CaCO_3$ which indicates a dilution controlled siliciclastic deposition sensu Ricken (1993), that is varying fine-grained siliciclastic input (mainly clay minerals and silt-sized quartz) controls the facies and cyclicity of the sediments, whereas the carbonate production stays fairly constant. The slope of the regression line of the dilution is moderately sloping, an indication of a small to moderate supply of organic matter in the background sediments. According to this model, decreasing amounts of organic carbon and carbonate in the sediment result from an increase in siliciclastic input and, consequently, indicate an increase in sedimentation rate. Detailed regression lines for various parts of the core display linear relationships (see Khatun 2007). Organic matter flux was limited to a threshold value around 0.8 % C_{org} . A slight change in deposition at depths of 55 to 70 m and at 70 to 85 m was recognized due to a flatter regression line from 55 to 70 m (Khatun 2007).

Type of organic matter based on Rock Eval pyrolysis

Rock Eval pyrolysis is used to identify the type and maturity of organic matter and to assess petroleum potential in sediments (e.g. Espitaliè et al. 1977) and can also be useful for paleoenvironmental reconstruction. The relatively high organic content of the Baden-Sooss core and the episodic lamination made us interested in learning more of the origin of the organic matter. The hydrogen index (HI) offers a way to estimate relative amounts of marine and terrestrial components building up the sedimentary organic matter. HI is the ratio of S2 to TOC given in milligrams of hydrocarbons for 1 g organic C (mg HC/g TOC). HI values range in general from around 30 to a maximum of 90 (Table 2), typical for type III kerogen which derived mainly from terrestrial higher plant material and only minor marine input, which is also indicated by the HI-OI diagram (Fig. 11). Rock Eval T_{max} values range around 410 to 425 with a maximum of 441 which indicates mainly immature conditions of the organic matter (Espitaliè et al. 1977).

Bulk geochemistry, mineralogy and clay mineralogy

Geochemical analysis for main elements largely corroborated the carbonate data given above. Although the geochemical composition of the samples is rather uniform (Table 3), samples rich in carbonate naturally have slightly lower silica values and vice versa. SiO_2 content ranges from 49.5 to 54.5 %. Outstanding is the tuff layer with a value of 57 %. CaO content ranges from 7.5% to 11.0 %; again the tuff layer shows a significantly different value of 4.2 %. Trace elements are also rather uniform throughout the core and show no significant variations. Even within the laminated part of the core around 85 m no concentration of anoxia-related elements like vanadium could be recognized (Table 3). The tuff naturally shows significant discrepancies, for example lower barium, chromium, strontium, and vanadium contents.

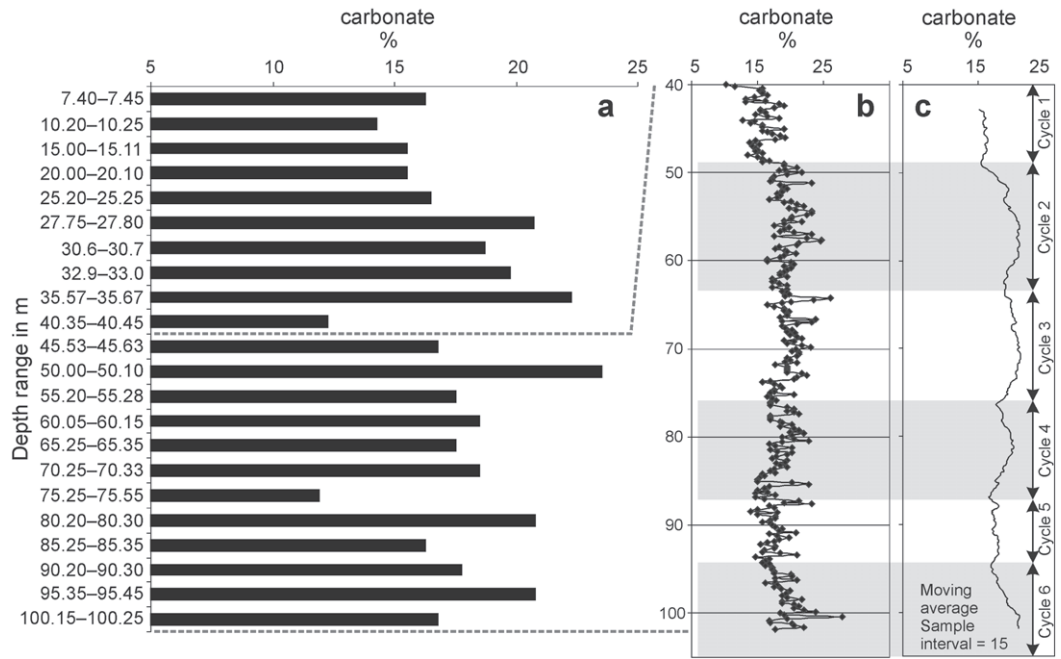


Fig. 8. Carbonate contents from (a) whole core overview samples, and (b) detailed sampling from 40 to 102 m. (c) moving average (sample interval = 15) shows cyclicity of the data.

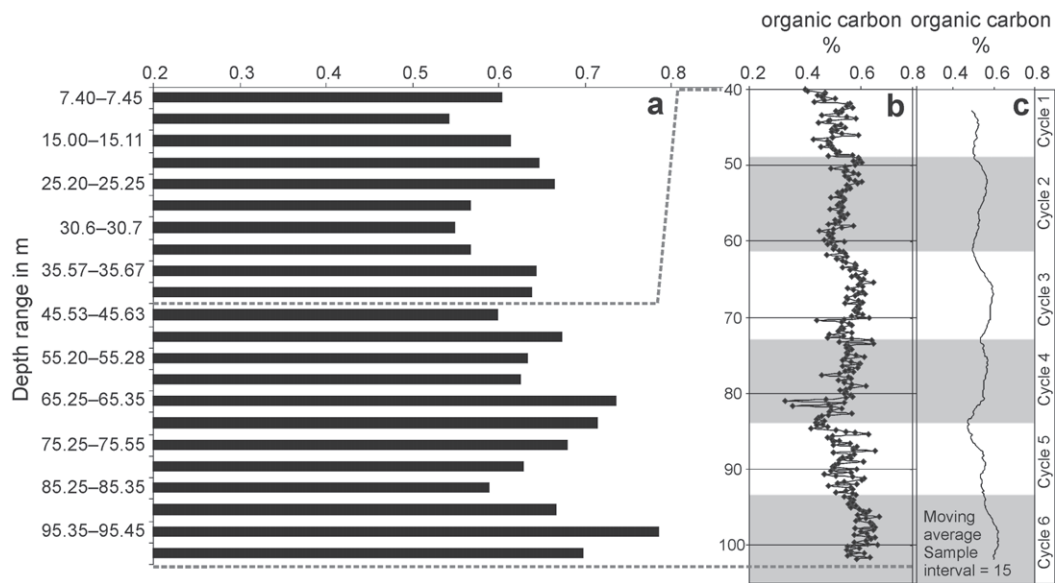


Fig. 9. Organic carbon contents from (a) whole core overview samples, and (b) detailed sampling from 40 to 102 m. (c) moving average (sample interval = 15) shows cyclicity of the data.

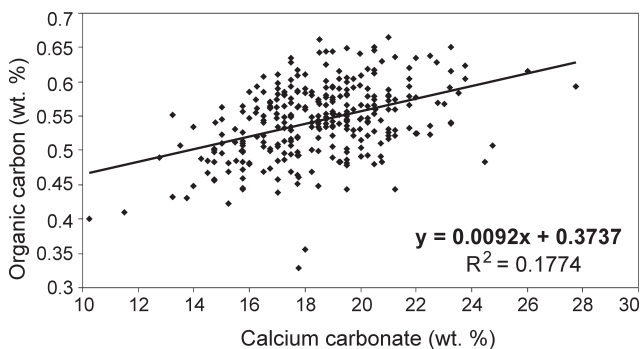


Fig. 10. C_{org} - $CaCO_3$ scatter diagram for the samples 40-102 m of the Baden-Sooss core displaying linear regression line.

The results of overview XRD analyses are shown in Fig. 12. Quartz, albite, muscovite/illite, chlorite, kaolinite, calcite and dolomite are the main mineral constituents. Pyrite is identified in all samples. The bulk mineralogy within the profile is rather uniform. The mineralogy of the samples was calculated on the basis of the geochemical bulk composition using the methods of Paktunc (1998). This indicates around 30 % of quartz, below 10 % of albite, 15-20 % of muscovite/illite, 10-15 % chlorite, 10 to 15 % of kaolinite, and 15-25 % of carbonate including dolomite. Decreasing amounts of carbonate correspond to an increase of siliciclastic components. Systematic variation in the relative abundance of any other mineral group was not observed. The clay minerals are considered to be detrital and supplied from the same source area of bedrocks and soils.

Table 2: TOC and Rock Eval data from 40–102 m of the Baden-Sooss core.

Depth (m)	TOC (wt. %)	S1 (mg/g)	S2 (mg/g)	S3 (mg/g)	T _{max} (°C)	HI (mg/g)
40.01	0.401	0.05	0.17	0.50	436	42.4
41.21	0.506	0.09	0.19	0.60	428	37.5
42.61	0.535	0.10	0.33	0.98	429	61.7
43.81	0.581	0.12	0.28	1.10	433	48.2
45.01	0.543	0.11	0.33	0.90	434	60.8
46.41	0.498	0.08	0.18	0.83	430	36.2
47.61	0.456	0.07	0.15	0.73	441	32.9
48.81	0.484	0.15	0.34	0.86	424	70.2
50.01	0.579	0.09	0.27	0.70	418	46.7
52.61	0.551	0.23	0.50	0.73	427	90.8
53.81	0.525	0.10	0.27	0.57	432	51.4
54.41	0.541	0.06	0.24	0.99	426	44.4
55.01	0.522	0.18	0.34	0.72	424	65.2
56.41	0.554	0.12	0.34	0.73	419	61.4
57.61	0.507	0.09	0.25	0.68	417	49.3
58.81	0.483	0.10	0.28	0.63	415	58.0
60.01	0.541	0.10	0.22	0.56	416	40.7
61.41	0.539	0.09	0.16	0.66	408	29.7
62.61	0.535	0.11	0.36	0.59	417	67.3
63.815	0.560	0.09	0.28	0.73	417	50.0
65.01	0.608	0.10	0.33	0.84	429	54.3
66.415	0.574	0.10	0.18	1.02	415	31.4
67.61	0.552	0.12	0.34	0.78	426	61.6
68.81	0.593	0.18	0.29	0.67	417	48.9
70.01	0.631	0.18	0.45	0.57	414	71.4
71.415	0.539	0.15	0.33	0.57	416	61.3
72.61	0.482	0.11	0.31	0.58	414	64.4
73.81	0.556	0.08	0.25	0.60	415	45.0
75.03	0.582	0.15	0.45	0.58	422	77.4
76.41	0.535	0.12	0.35	0.77	424	65.4
77.61	0.459	0.08	0.17	0.51	437	37.1
77.63	0.459	0.10	0.30	0.57	415	65.4
78.81	0.567	0.12	0.37	0.66	423	65.3
78.83	0.567	0.12	0.32	0.63	419	56.4
80.01	0.540	0.16	0.36	0.40	401	66.7
81.41	0.485	0.15	0.38	0.68	411	78.4
82.61	0.567	0.08	0.32	0.95	434	56.5
83.815	0.439	0.05	0.15	0.59	409	34.2
84.385	no data	0.08	0.21	0.70	426	no data
84.415	0.480	0.09	0.28	0.70	419	58.3
85.03	0.545	0.09	0.31	0.63	416	56.9
86.43	0.502	0.05	0.23	0.50	412	45.9
87.63	0.651	0.03	0.22	0.78	420	33.8
88.83	0.524	0.05	0.20	0.90	418	38.2
90.01	0.586	0.11	0.42	0.65	421	71.7
91.43	0.604	0.03	0.24	0.90	428	39.7
92.64	0.570	0.04	0.34	0.82	423	59.7
93.83	0.547	0.07	0.39	0.73	419	71.4
95.03	0.564	0.09	0.47	0.54	416	83.3
95.43	0.629	0.07	0.44	0.67	423	70.0
96.23	0.665	0.05	0.38	0.89	420	57.2
96.43	0.617	0.08	0.35	0.79	429	56.8
97.235	0.643	0.08	0.48	0.74	417	74.7
97.63	0.650	0.07	0.45	0.81	424	69.3
98.03	0.644	0.10	0.56	0.67	424	87.0
100.01	0.661	0.12	0.55	0.73	423	83.2
101.03	0.611	0.09	0.46	0.68	424	75.3
101.43	0.553	0.07	0.25	0.75	426	45.2
101.63	0.634	0.08	0.26	0.90	420	41.0

The clay minerals of the < 2 µm fraction comprise abundant illite/muscovite associated with fairly abundant amounts of chlorite and kaolinite. A low intensity, broad peak at angles between 3 and 4.2° 2θ indicates the presence of a mixed layer, which could not be further identified. Smectite abundance

varies most. A decrease upward can be recognized from a maximum at 70 to 75 m to accessory amounts in the upper 50 m of the section. The clay mineralogy of the tuff layer is dominated by low charged smectite with traces of illite, chlorite and kaolinite. Small amounts of quartz, albite, calcite, dolomite and pyrite occur in the bulk mineralogy.

Magnetic susceptibility

Selge (2005) recognized mixed assemblages of multiple magnetic fractions in the core samples with different grain sizes and mineralogy such as magnetite, maghaemite, hematite, goethite, and pyrite. The results of thermomagnetic investigations indicated magnetite as the dominant magnetic phase in all studied samples with additional presence of varying amounts of hematite (for details see Selge 2005). Magnetic susceptibility measured on the full length of the core indicated cyclic variations with a highly significant large scale cycle of about 40 m and small scale cycles of about 20, 15 and 11 m in thickness (Fig. 13 and Hohenegger et al. 2008a). Peaks in magnetic susceptibilities were linked to higher concentration of hematite related to higher sediment influx as a consequence of higher seasonal contrasts (cold winters and hot summers). These enhanced climate variations resulted in higher rates of physical weathering and erosion and, consequently, a higher amount of detrital magnetic particles deposited in the basin (Selge 2005; Hohenegger et al. 2008a).

Discussion

The lithofacies and biofacies of the marls and clays of the Badenian stratotype were interpreted by Papp & Steininger (1978) as a shallow-water, fully-marine, basinal fine-grained facies of water depths around 50–100 m. Sand and shell layers were interpreted as higher energy layers transported from more nearshore environments to the west into the calm depositional environment (Papp & Steininger 1978).

According to our investigations, the Baden-Sooss core strata were deposited within a quiet offshore depositional environment as proven by the predominance of fine silt and clay grain sizes of the typical “Badener Tegel”. Depositional waterdepths were situated below the fair-weather wave base as no structures indicative of wave agitation have been found. Bioturbation is common, also characteristic for moderately deep environments below the normal wave base (see Pervesler et al. 2008). The poor sorting indicated by grain size analysis may be mainly a result of strong bioturbation. The fine median values from grain size analysis and the CM-plots indicate transport and sedimentation from pelagic suspension; no evidence for turbiditic transport for these fine-grained sediments is present.

Table 3: Main element (in weight %) and trace element (in ppm) geochemistry of samples from the Baden-Sooss core.

Sample from core meter	7 m	10 m	15 m	20 m	25 m	30 m	35 m	40 m	45 m	50 m	55 m
SiO ₂	53.0	54.5	54.0	54.0	54.5	53.0	50.0	53.5	52.5	50.0	52.0
TiO ₂	0.743	0.773	0.726	0.764	0.732	0.665	0.679	0.734	0.740	0.686	0.694
Al ₂ O ₃	15.90	16.50	15.50	16.40	15.10	13.75	14.10	15.70	15.70	14.45	14.47
Fe ₂ O ₃	4.80	4.60	4.40	4.50	4.40	4.00	4.40	4.50	4.80	4.20	4.00
MnO	0.048	0.059	0.051	0.054	0.045	0.047	0.050	0.066	0.064	0.053	0.050
MgO	2.10	2.00	2.10	2.00	2.15	2.10	2.25	2.45	2.05	2.00	2.20
CaO	8.50	7.50	8.30	7.60	8.00	10.50	11.00	8.50	9.00	11.00	10.50
Na ₂ O	0.80	1.17	1.16	1.19	1.12	1.32	1.11	1.03	1.37	1.08	1.17
K ₂ O	2.53	2.70	2.39	2.69	2.41	2.19	2.39	2.54	2.54	2.32	2.34
H ₂ O _{110 °C}	1.36	1.31	1.28	1.37	1.25	0.99	1.08	1.24	1.19	1.17	1.19
P ₂ O ₅	0.103	0.113	0.099	0.151	0.095	0.077	0.106	0.095	0.122	0.116	0.104
CO ₂	9.10	8.40	9.60	8.90	9.70	10.80	12.30	8.80	9.80	12.60	11.20
SO ₃	1.12	0.40	0.32	0.50	0.45	0.46	0.33	0.60	0.25	0.45	0.29
total	100.11	100.03	99.92	100.12	99.95	99.90	99.80	99.75	100.12	100.13	100.21
Ba	256	279	259	281	270	233	269	290	277	266	276
Co	18	19	15	18	12	13	15	19	19	15	14
Cr	117	134	140	137	130	145	142	134	132	124	117
Cs	7	10	8	12	7	6	4	8	6	8	6
Cu	47	54	45	54	48	40	43	52	57	45	42
Ni	56	59	52	59	55	48	52	55	58	57	49
Pb	21	23	21	24	21	19	20	22	23	20	21
Rb	128	142	126	142	128	109	121	128	135	119	121
Sr	251	227	255	260	254	278	311	276	278	292	328
V	133	145	127	148	136	104	119	129	138	129	119
Y	23	24	24	24	24	22	23	23	23	22	22
Zn	89	98	88	98	89	79	84	90	93	83	83
Zr	163	162	186	152	181	190	169	180	160	158	178
total	1311	1376	1347	1409	1354	1285	1371	1406	1398	1338	1375
Sample from core meter	60 m	65 m	70 m	75 m	80 m	85 m	90 m	95 m	100 m	Tuff	
SiO ₂	51.5	52.0	51.0	51.0	49.5	53.0	51.0	49.5	52.0	57.0	
TiO ₂	0.708	0.695	0.666	0.698	0.688	0.748	0.730	0.697	0.727	0.411	
Al ₂ O ₃	14.97	14.77	14.33	15.03	14.97	15.91	15.33	14.95	15.64	18.48	
Fe ₂ O ₃	4.10	4.40	4.00	4.20	4.70	4.50	4.10	4.30	4.20	3.65	
MnO	0.044	0.049	0.045	0.049	0.054	0.062	0.052	0.048	0.050	0.022	
MgO	2.13	2.16	2.16	2.30	2.27	2.39	2.13	2.24	2.35	2.23	
CaO	10.00	9.60	10.50	9.80	10.30	8.15	9.85	10.50	9.00	4.20	
Na ₂ O	1.20	1.15	1.43	1.34	1.36	1.28	1.39	1.34	1.32	1.73	
K ₂ O	2.48	2.41	2.32	2.48	2.48	2.68	2.56	2.49	2.60	1.35	
H ₂ O _{110 °C}	1.20	1.28	1.30	1.19	1.16	1.21	1.21	1.24	1.24	5.64	
P ₂ O ₅	0.137	0.096	0.100	0.097	0.119	0.103	0.120	0.139	0.125	0.049	
CO ₂	10.90	11.00	11.85	11.35	12.20	9.70	11.00	12.10	10.50	4.90	
SO ₃	0.50	0.46	0.50	0.53	0.38	0.29	0.42	0.60	0.42	0.32	
total	99.86	100.07	100.20	100.05	100.18	100.02	99.88	100.14	100.18	99.97	
Ba	291	295	277	290	305	316	320	305	312	189	
Co	17	16	15	17	12	14	15	17	14	13	
Cr	113	123	124	130	125	132	117	125	131	62	
Cs	11	8	11	7	8	6	12	9	7	3	
Cu	44	42	40	44	46	55	48	45	47	32	
Ni	50	54	50	59	54	62	57	53	53	34	
Pb	21	21	19	20	21	24	22	20	22	28	
Rb	126	124	118	127	130	142	134	131	136	69	
Sr	360	331	334	309	337	282	324	347	313	285	
V	128	115	123	124	133	139	142	132	139	68	
Y	24	23	22	23	22	23	23	22	24	21	
Zn	86	84	81	86	87	96	89	88	90	80	
Zr	163	175	177	172	150	150	159	150	159	165	
total	1433	1410	1393	1408	1430	1441	1462	1443	1447	1048	

Ubiquitous bioturbation generally indicates oxic bottom water conditions except for minor primary laminated intervals, which can be related to dysoxic conditions. The laminae are partly disturbed by trace fossils due to subsequent improvement of oxygenation and burrowing. The trace fossil *Scolicia*, produced by stenohaline irregular echinoids, indi-

cates full marine conditions (e.g. Bromley & Asgaard 1975; Smith & Crimes 1983). The salinity tolerant crustacean burrow *Thalassinoides* (Frey et al. 1984) replaces *Scolicia* in the higher portions of the core. The presence of *Zoophycos* and associated *Phycosiphon*, *Nereites* and *Teichichnus* suggests the *Zoophycos* ichnofacies for the deeper part of the core. Up

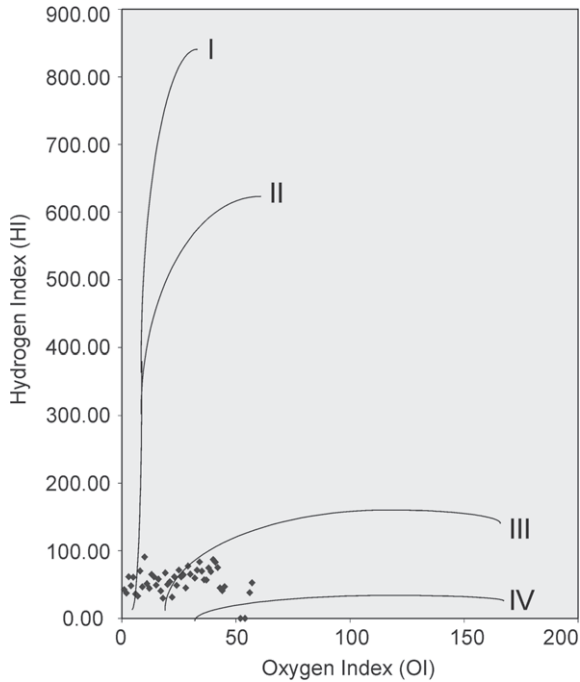


Fig. 11. Hydrogen Index (HI) versus Oxygen Index (OI) diagram based on Rock Eval analysis for samples from 40–102 m; kerogen types I–IV based on Espitaliĉ et al. (1977).

the core, *Thalassinoides* is more common. This may suggest a transition to the distal *Cruziana* ichnofacies. Such a relation indicates shallowing up to the upper offshore zone (cf. Pemberton et al. 2001) or at least a higher clastic input.

The percentage of carbonate of 10 % and 35 % indicates the presence of marls. XRD analysis shows mainly calcite, dolomite contents are rather low in percentage. The carbonate contents in such a fully marine, deeper-water setting may include the following constituents:

- Pelagic carbonate from the tests of mainly planktonic, carbonate secreting organisms (mainly calcareous nannoplankton and foraminifera);
- Reworked extra-basinal carbonate from the erosion of carbonate rocks in the hinterland of the basin;
- Minor constituents include carbonate from shells and tests of benthic organisms (e.g. molluscs, foraminifera) and authigenic carbonate precipitated on the sea floor or during diagenesis.

The main carbonate constituents as seen in the Baden-Sooss core samples are calcareous nannofossils, planktonic and benthic foraminifera (see Ćorić & Hohenegger 2008) and some mollusc shells. Presence of extra basinal, reworked carbonate could be excluded or is at least below 10 % in the fine-grained parts of the core, due to the lack of significant amounts of dolomite. Thus, the ‘Baden Tegel’ can be classified as a hemipelagite, namely a mixture of mainly pelagic

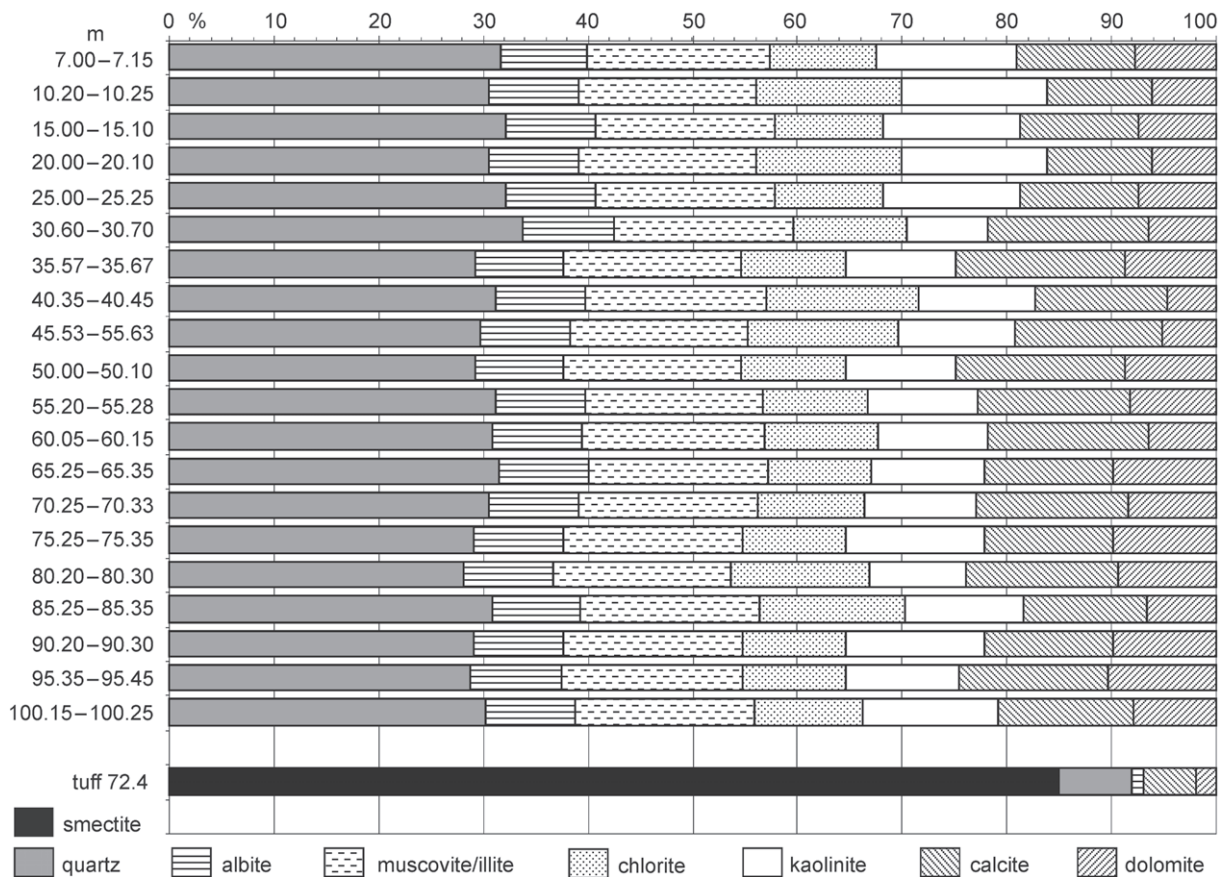


Fig. 12. Bulk mineral composition of 20 core samples and the tuff layer.

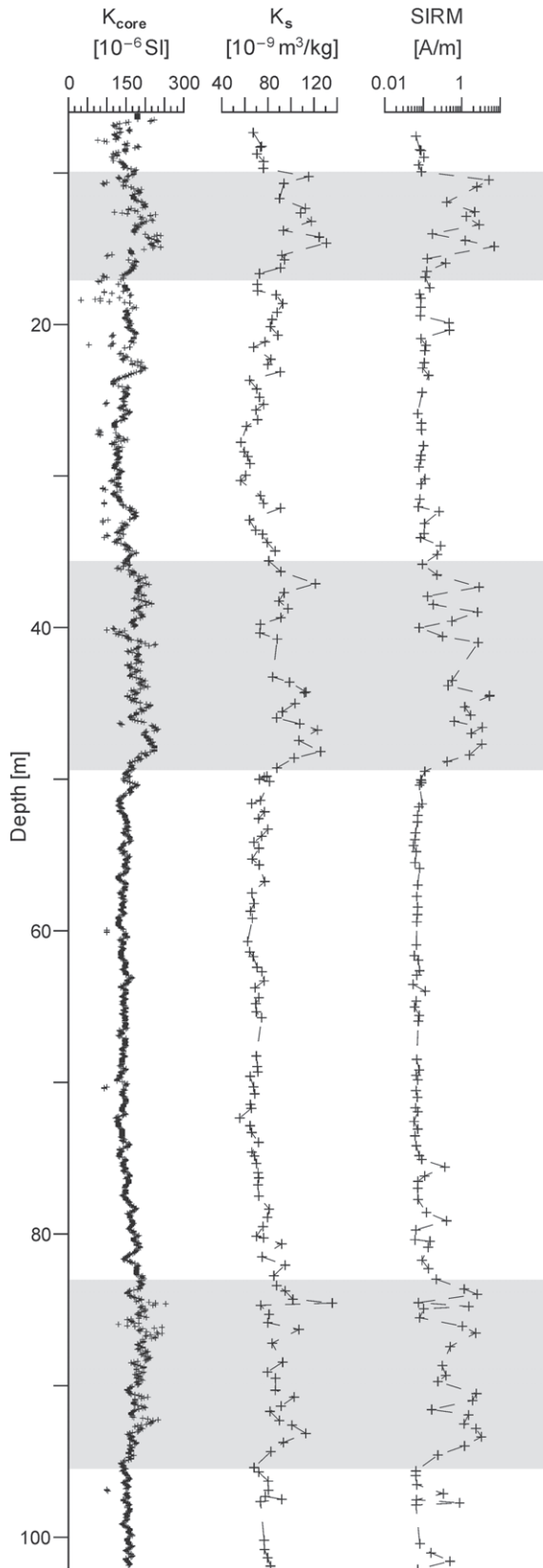


Fig. 13. Magnetic susceptibility, measured on the core (κ_{core}) and on subsamples (κ_s); the SIRM ratios describe the relative contributions of high-coercive to low-coercive magnetic phases (for details see Selge 2005). Cycle peaks (grey) identified by high values of susceptibility.

biogenic carbonate and terrigenous clay and silt. The presence of muscovite and chlorite in the clay mineral suite points to significant amounts of metamorphic source areas, that is the Austroalpine basement units to the south and east of the Vienna Basin. No systematic variations in the length of the core have been recognized in the composition of the detrital fraction, indicating neither provenance changes nor major climate changes during this interval.

The organic matter fraction of fine-grained sediments can be composed of organic particles of various sources, including imported terrestrial plant matter and matter primarily produced in the marine environment. The accumulation of organic matter in depositional environments is controlled by three main variables: rates of production, destruction, and dilution (Bohacs et al. 2005). The distribution and concentration of organic carbon through the analysed core indicates that organic matter flux was limited to a threshold value below 0.8 % C_{org} . Consequently, the rates of production of organic matter were comparatively low. The whole data set generally follows a dilution controlled siliciclastic flux model (sensu Ricken 1993) with moderate to low levels of production and minor destruction of organic matter.

This depositional type, characterized by varying siliciclastic input, suggests a hemipelagic, oxic environment. No signs for anoxia were found even in laminated parts of the core. The hydrogen index and oxygen data of Rock Eval analysis mainly suggest a terrestrial plant material source for the organic matter mixed with marine organic matter. The hydrogen index versus oxygen index plot demonstrates kerogen type III, though a very few samples show a minor tendency for type II kerogen of marine production. The plot also indicates an immature stage of hydrocarbon generation.

The low slope or flatness of the carbonate-organic carbon regression lines support the interpretation of a varying siliciclastic dominated background sedimentation with minor admixtures in pelagic biogenic carbonate. The siliciclastics are derived from continental fluvial input into the basin. Periods with high carbonate production are predominantly associated with higher oxygenation at the sediment surface, expressed in a decreasing supply of organic matter. Decreasing amounts of organic carbon and carbonate in the sediment suggest an increase in the sedimentation rate (Ricken 1996).

The results presented can also be interpreted in terms of subtle variations in relative sea level and productivity. Intervals with lower carbonate contents might represent regressional or sea-level lowstand phases characterized by low calcareous productivity and high siliciclastic dilution. These could be associated with higher runoff from the rising orogenic hinterland. Times of high sea level may thus result in lower siliciclastic dilution and higher plankton productivity.

Infrequent sand and shell layers, also strongly bioturbated, record the effect of higher energy events, probably storms, and thus can be interpreted as tempestites transported from near-shore or deltaic environments to the west. They may also represent distal pro-delta sand layers (comp. Wessely et al. 2007). Due to the lack of primary sedimentary structures both interpretations are still valid; deposition above or within the storm wave base can be assumed due to the presence of shell lags. The slight increase in number of sand layers towards the upper

part of the core indicates shallowing or a higher sand input. A slight shallowing in the uppermost part of the section is also indicated by the increase in number of macrofossil lenses as described from the stratotype section (Papp & Steininger 1978) and is corroborated by the trace fossil record (Pervesler et al. 2008) and foraminiferal assemblages (Hohenegger et al. 2008b). A general shallowing trend in largely coeval Badenian sediments was also recorded a few kilometers further to the south, at Bad Vöslau (Wessely et al. 2007).

Rare events disturbing the generally quiet offshore sedimentation of fine-grained sediments include a debris flow conglomerate bed in the upper part of the core. This submarine mass flow may have been triggered by seismic shocks due to earthquakes at nearby synsedimentary basin margin faults. A tuff layer in the lower part of the core testifies to the presence of coeval volcanism some distance away from the Vienna Basin (see, e.g. Handler et al. 2006).

Conclusion

From grain size analysis and geochemical data of the Baden-Sooss core at the type locality of the Badenian we conclude that the fine-grained bioturbated deposits of the southern Vienna Basin were deposited in a quiet offshore environment below the fair weather wave base. A pelagic autochthonous carbonate fraction, mainly calcareous nanofossils and foraminifera, and a terrigenous clay and fine silt fraction form the marls of the "Badener Tegel". Cyclic sedimentation was mainly due to variance in the siliciclastic input, that is dilution cycles due to siliciclastic-dominated flux. Organic matter derived mainly from terrigenous input of higher land plants. A slight shallowing is recorded from the lower to the upper part of the core.

Acknowledgments: The study was supported by the Austrian Science Fund (FWF, Projects P13743-BIO, P13740-GEO, P18203-N10 and P16793-B06). We thank Alfred Uchman, Katalin Báldi, Stjepan Ćorić, Fred Rögl, Christian Rupp, Anna Selge, Robert Scholger and Karl Stingl for assistance and helpful discussions. We thank the technical staff of the Department of Paleontology, University of Vienna, for transporting and cutting the core. We thank Maria Fencl for preparation of sedimentological logs. We thank the reviewers of the manuscript for suggestions and improvements.

References

- Blott S.J. & Pye K. 2001: Gradistat: a grain size distribution and statistics package for the analysis of unconsolidated sediments. *Earth Surf. Process. Landforms* 26, 1237–1248.
- Bohacs K.M., Grabowski G.J., Carroll A.R., Mankiewicz P.J., Miskell-Gerhardt K.J., Schwalbach J.R., Wegner M.B. & Simo J.A. 2005: Production, destruction, and dilution — the many paths to source-rock development. In: Harris N.B. (Ed.): The deposition of organic-carbon-rich sediments: models, mechanisms, and consequences. *SEPM Spec. Publ.* 82, 61–101.
- Brix F. & Plöschinger B. 1988: Erläuterungen zu Blatt Wiener Neustadt. *Geol. Bundesanst.*, Wien, 1–85.
- Bromley R.G. & Asgaard U. 1975: Sediment structures produced by a spatangoid echinoid: a problem of preservation. *Bull. Geol. Soc. Denmark* 24, 261–281.
- Ćorić S. & Hohenegger J. 2008: Quantitative analyses of calcareous nannoplankton assemblages from the Baden-Sooss section (Middle Miocene of Vienna Basin, Austria). *Geol. Carpathica* 59, 5, 447–460.
- Decker K. 1996: Miocene tectonics at the Alpine-Carpathian junction and the evolution of the Vienna Basin. *Mitt. Gesell. Geol. Bergbaustud. Österr.* 41, 33–44.
- d'Orbigny A. 1846: Foraminifères fossiles du Bassin Tertiaire de Vienne (Autriche). Die fossilen Foraminiferen des tertiären Beckens von Wien. *Gide et Comp.*, Paris, I–XXXVII, 1–312.
- Espitaliè J., LaPorte J.L., Madec M., Marquis F., Leplat P., Paulet J. & Boutefeu A. 1977: Méthode rapide de caractérisation des roches mères de leur potentiel pétrolier et de leur degré d'évolution. *Rev. Inst. Français Pétrole* 32, 23–42.
- Folk R.L. & Ward W.C. 1957: Brazos River bar (Texas); a study in the significance of grain size parameters. *J. Sed. Petrology* 27, 3–26.
- Frey R.W., Curran A.H. & Pemberton G.S. 1984: Tracemaking activities of crabs and their environmental significance: the ichnogenus *Psilonichnus*. *J. Paleontology* 58, 511–528.
- Grill R. 1941: Stratigraphische Untersuchungen mit Hilfe von Mikrofaunen im Wiener Becken und den benachbarten Molasse-Anteilen. *Öl Kohle* 37, 595–602.
- Grill R. 1943: Über mikropaläontologische Gliederungsmöglichkeiten im Miozän des Wiener Becken. *Mitt. Reichsanstalt für Bodenforschung* 6, 33–44.
- Hamilton W., Wagner L. & Wessely G. 2000: Oil and gas in Austria. *Mitt. Österr. Geol. Gesell.* 92, 235–262.
- Handler R., Ebner F., Neubauer F., Bojar A.-V. & Hermann S. 2006: $^{40}\text{Ar}/^{39}\text{Ar}$ dating of Miocene tuffs from the Styrian part of the Pannonian Basin: an attempt to refine the basin stratigraphy. *Geol. Carpathica* 57, 483–494.
- Hardenbol J., Thierry J., Farley M.B., Jacquin T., Graciansky P.-C. & Vail P.R. 1998: Mesozoic and Cenozoic sequence chronostratigraphic framework of European basins. In: Graciansky P.-C., Hardenbol J., Jacquin T. & Vail P.R. (Eds.): Mesozoic and Cenozoic sequence stratigraphy of European basins. *SEPM Spec. Publ.* 60, 3–13.
- Harzhauser M. & Piller W.E. 2005a: Neogen des Wiener Beckens. *Exkursionsführer 75. Jahrestagung der Paläontologischen Gesellschaft*, Graz, 1–42.
- Harzhauser M. & Piller W.E. 2005b: Paratethyan paleogeography depositional regimes and major sea-level fluctuations. *Excursion A., 12th Congress R.C.M.N.S., 6–11. September 2005, Vienna, 6–11.*, Vienna.
- Harzhauser M. & Piller W.E. 2007: Benchmark data of a changing sea — Palaeogeography, palaeobiogeography and events in the Central Paratethys during the Miocene. *Palaeogeogr. Palaeoclimatol. Palaeoecol.* doi:10.1016/j.palaeo.2007.03.031.
- Hámor G. 2001: Explanatory notes to the Miocene palaeogeographic maps of the Carpathian Basin. *Geol. Inst. Hung.*, Budapest, 1–71.
- Hinsch R., Decker K. & Wagrreich M. 2005: 3-D mapping of segmented active faults in the southern Vienna Basin. *Quart. Sci. Rev.* 24, 321–336.
- Hohenegger J., Ćorić S., Khatun M., Pervesler P., Rögl F., Rupp C., Selge A., Uchman A. & Wagrreich M. 2008a: Cyclostratigraphic dating in the Lower Badenian (Middle Miocene) of the Vienna Basin (Austria) — the Baden-Sooss core. *Int. J. Earth Sci.* DOI 10.1007/s00531-007-0287-7.
- Hohenegger J., Andersen N., Báldi K., Ćorić S., Pervesler P., Rupp C. & Wagrreich M. 2008b: Paleoenvironment of the Early Badenian (Middle Miocene) in the southern Vienna Basin (Aus-

- tria) — multivariate analysis of the Baden-Sooss section. *Geol. Carpathica* 59, 5, 461–487.
- Hörnes M. 1856: Die fossilen Mollusken des Tertiärbeckens von Wien (Gastropoden). *Abh. Geol. Reichsanst. Wien* 3, 1–404.
- Hörnes M. 1870: Die fossilen Mollusken des Tertiärbeckens von Wien (Bivalven). *Abh. K.K. Geol. Reichsanst. Wien* 4, 1–279.
- Karrer F. 1867: Zur Foraminiferenfauna in Österreich. *Sitz.-Ber. K.K. Akad. Wiss., Math. Naturwiss. Cl.* 55, 331–368.
- Keferstein C. 1828: Beobachtungen und Ansichten über die geognostischen Verhältnisse der nördlichen Kalk-Alpenkette in Oesterreich und Baiern. *Deutschland Geognostisch-Geol. Dargestellt* 5, (3), 1–425.
- Kováč M., Baráth I., Harzhauser M., Hlavatý I. & Hudáčková N. 2004: Miocene depositional systems and sequence stratigraphy of the Vienna Basin. *Cour. Forsch.-Inst. Senckenberg* 246, 187–212.
- Kvaček Z., Kováč M., Kovar-Eder J., Doláková N., Jechorek H., Parashiv V., Kováčová M. & Sliva L. 2006: Miocene evolution of landscape and vegetation in the Central Paratethys. *Geol. Carpathica* 57, 4, 295–310.
- Lankreijer A., Kováč M., Cloetingh S., Pitoňák P., Hlůška M. & Biermann C. 1995: Quantitative subsidence analysis and forward modelling of the Vienna and Danube basins; thin-skinned versus thick-skinned extension. *Tectonophysics* 252, 433–451.
- Lourens L., Hilgen F., Shackleton N.J., Laskar J. & Wilson D. 2004: The Neogene Period. In: Gradstein F.M., Ogg J.G. & Smith A.G. (Eds.): A geologic time scale 2004. *Cambridge Univ. Press*, 409–440.
- Moore D.M. & Reynolds R.C. 1997: X-ray diffraction and the identification and analysis of clay minerals. 2nd Edition. *Oxford University Press*, New York, 1–378.
- Müller G. & Gastner M. 1971: The “Karbonat-Bombe,” a simple device for the determination of the carbonate content in sediments, soils and other materials. *Neu. Jb. Mineral., Mh.* 10, 466–469.
- Paktunc A.D. 1998: Modan: an interactive computer program for estimating mineral quantities based on bulk composition: windows version. *Computers and Geosciences* 24, 425–431.
- Papp A. 1951: Das Pannon des Wiener Beckens. *Mitt. Geol. Gesell.* 39–41 (1946–48), 99–193.
- Papp A. 1953: Die Molluskenfauna des Pannon im Wiener Becken. *Mitt. Geol. Gesell.* 44, 85–222.
- Papp A. & Steininger F. 1978: Holostratotypus des Badenien. Holostratotypus: Baden-Sooss (südlich von Wien), Niederösterreich, Österreich. Badener Tegel-Keferstein, 1828 (Unterbaden; M4b; Obere Lagenidenzone). In: Papp A., Cicha I., Seneš J. & Steininger F. (Eds.): Chronostratigraphie und Neostratotypen: Miozän der Zentralen Paratethys. Bd. VI. M₄ Badenien (Moravien, Wielicien, Kosovien). *VEDA SAV*, Bratislava, 138–145.
- Papp A., Grill R., Janoschek R., Kapounek J., Kollmann K. & Turnovsky K. 1968: Zur Nomenklatur des Neogens in Österreich — Nomenclature of the Neogene of Austria. *Verh. Geol. Bundesanst.* 1968, 9–27.
- Papp A., Cicha I., Seneš J. & Steininger F. (Eds.) 1978: Chronostratigraphie und Neostratotypen: Miozän der Zentralen Paratethys. Bd. VI. M₄ Badenien (Moravien, Wielicien, Kosovien). *VEDA SAV*, Bratislava, 1–594.
- Passega R. 1964: Grain size representation by CM patterns as a geologic tool. *J. Sed. Petrology* 34, 830–847.
- Pemberton S.G., Spila M., Pulham A.J., Saunders T., MacEachern J.A., Robbins D. & Sinclair I.K. 2001: Ichnology and sedimentology of shallow to marginal marine systems. *Geol. Assoc. Canada, Short Course Notes* 15, 1–343.
- Pervesler P., Uchman A. & Hohenegger J. 2008: New methods for ichnofabric analysis and correlation with orbital cycles exemplified by the Baden-Sooss section (Middle Miocene, Vienna Basin). *Geol. Carpathica* 59, 5, 395–409.
- Piller W.E., Egger H., Erhart C., Gross M., Harzhauser M., Hubmann B., van Husen D., Krenmayr H.-G., Krystyn L., Lein R., Lukeneder A., Mandl G., Rögl F., Roetzel R., Rupp C., Schnabel W., Schönlaub H.P., Summesberger H. & Wagneich M. 2004: Die Stratigraphische Tabelle von Österreich 2004 (sedimentäre Schichtfolgen). Österreichische stratigraphische Kommission und Kommission für die paläontologische und stratigraphische Erforschung Österreichs.
- Ratschbacher L., Frisch W., Linzer H.G. & Merle O. 1991: Lateral extrusion in the Eastern Alps. 2. Structural analysis. *Tectonics* 10, 257–271.
- Reuss A.E. 1848: Die fossilen Polyparien des Wiener Tertiärbeckens. *Naturwiss. Abh. von W. Heidinger* 2, 1–78.
- Ricken W. 1991: Variations of sedimentation rates in rhythmically bedded sediments. Distinction between depositional types. In: Einsele G., Ricken W. & Seilacher A. (Eds.): Cycles and events in stratigraphy. *Springer*, Berlin, 168–187.
- Ricken W. 1993: Sedimentation as a three-component system. *Lecture N. Earth Sci.* 51, 1–211.
- Ricken W. 1996: Bedding rhythms and cyclic sequences as documented in organic carbon-carbonate patterns, Upper Cretaceous, Western Interior, U.S. *Sed. Geol.* 102, 131–154.
- Royden L.H. 1985: The Vienna Basin. A thin-skinned pull-apart basin. In: Biddle K.T. & Christie-Blick N. (Eds.): Strike slip deformation, basin formation and sedimentation. *SEPM Spec. Publ.* 37, 319–338.
- Rögl F. 1998: Palaeogeographic considerations for Mediterranean and Paratethys seaways (Oligocene to Miocene). *Ann. Naturhist. Mus. Wien* 99A, 279–310.
- Rögl F. 1999: Mediterranean and Paratethys, facts and hypotheses of an Oligocene to Miocene paleogeography (short overview). *Geol. Carpathica* 50, 4, 339–349.
- Rögl F., Čorić S., Harzhauser M., Jiménez-Moreno G., Kroh A., Schultz O., Wessely G. & Zorn I. 2008: The Middle Miocene Badenian stratotype at Baden-Sooss (Lower Austria). *Geol. Carpathica* 59, 5, 367–374.
- Sauer R., Seifert P. & Wessely G. 1992: Guidebook to Excursions in the Vienna Basin and the adjacent Alpine-Carpathian thrustbelt in Austria. *Mitt. Österr. Geol. Gesell.* 85, 1–264.
- Seifert P. 1996: Sedimentary-tectonic development and Austrian hydrocarbon potential of the Vienna Basin. In: Wessely G. & Liebl W. (Eds.): Oil and gas in Alpidic thrustbelts and basins of Central and Eastern Europe. *EAGE Spec. Publ., (Geol. Soc. London)* 5, 331–341.
- Selge A. 2005: Cyclostratigraphy by means of mineralmagnetic parameters in the middle Badenian (Middle Miocene) core Soos/Baden (Vienna Basin, Austria). *Unpubl. Dipl. Thesis, University of Leoben*, 1–84.
- Smith A.B. & Crimes T.P. 1983: Trace fossils formed by heart urchins — a study of *Scolicia* and related traces. *Lethaia* 16, 79–92.
- Steininger F.F. & Papp A. 1979: Current biostratigraphic and radiometric correlations of Late Miocene Central Paratethys stages (Sarmatian s.str., Pannonian s.str. and Pontian) and Mediterranean stages (Tortonian and Messinian) and the Messinian Event in the Paratethys. *Newslett. Stratigr.* 8, 100–110.
- Strauss P., Harzhauser M., Hirsch R. & Wagneich M. 2006: Sequence stratigraphy in a classical pull-apart basin (Neogene, Vienna Basin). A 3D seismic based integrated approach. *Geol. Carpathica* 57, 185–197.
- Wagner J.-F. & Czurda K.A. 1991: Radionuklidsorption an tertiären Tonen. *Mitt. Österr. Geol. Gesell.* 83, 215–227.
- Wagneich M. & Schmid H.P. 2002: Backstripping dip-slip fault histories: Apparent slip rates for the Miocene of the Vienna Basin. *Terra Nova* 14, 163–168.
- Weissenböck M. 1996: Lower to Middle Miocene sedimentation

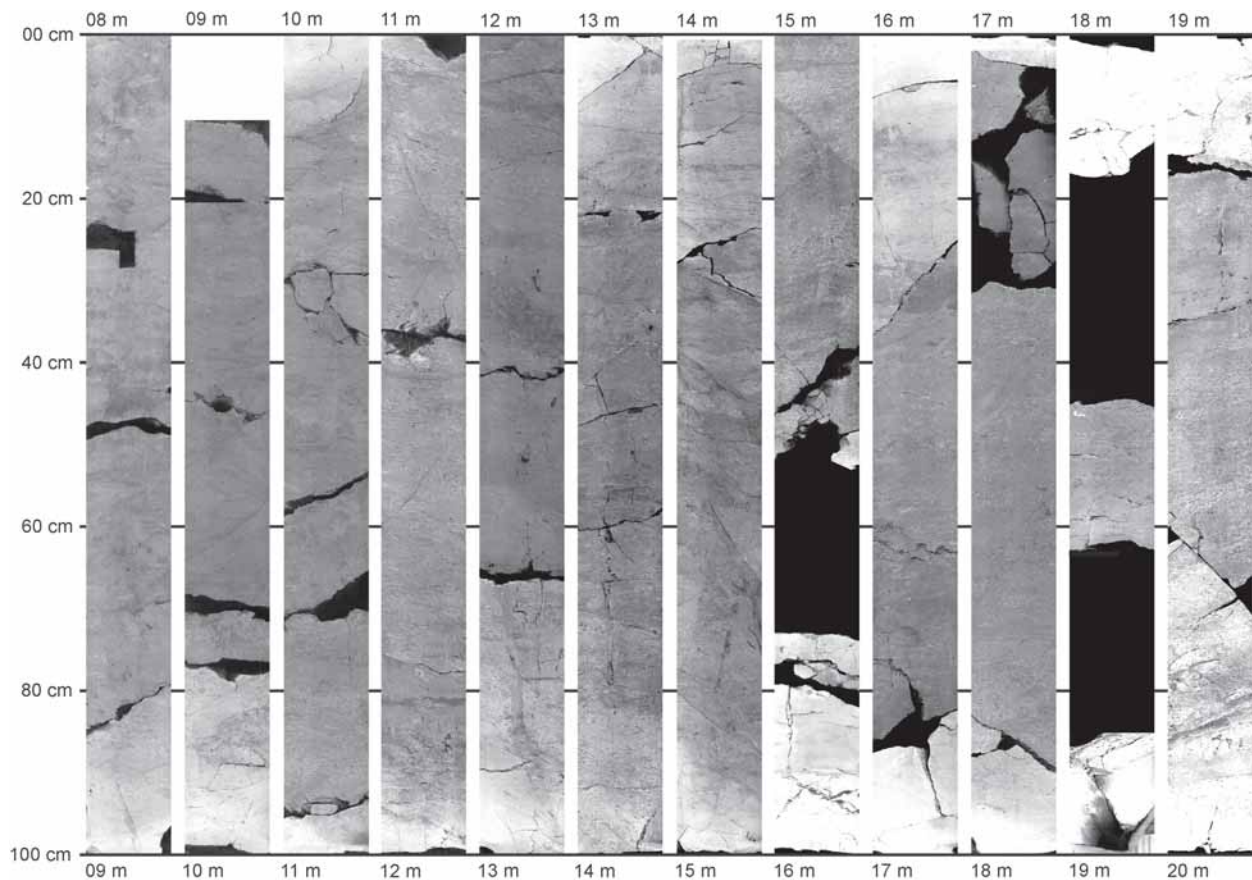
model of the central Vienna Basin. In: Wessely G. & Liebl W. (Eds.): Oil and gas in Alpidic thrustbelts and basins of Central and Eastern Europe. *EAGE Spec. Publ. 5*, 255–363.

Wessely G. 1988: Structure and development of the Vienna Basin in Austria. In: Royden L.H. & Horvath F. (Eds.): The Pamponian

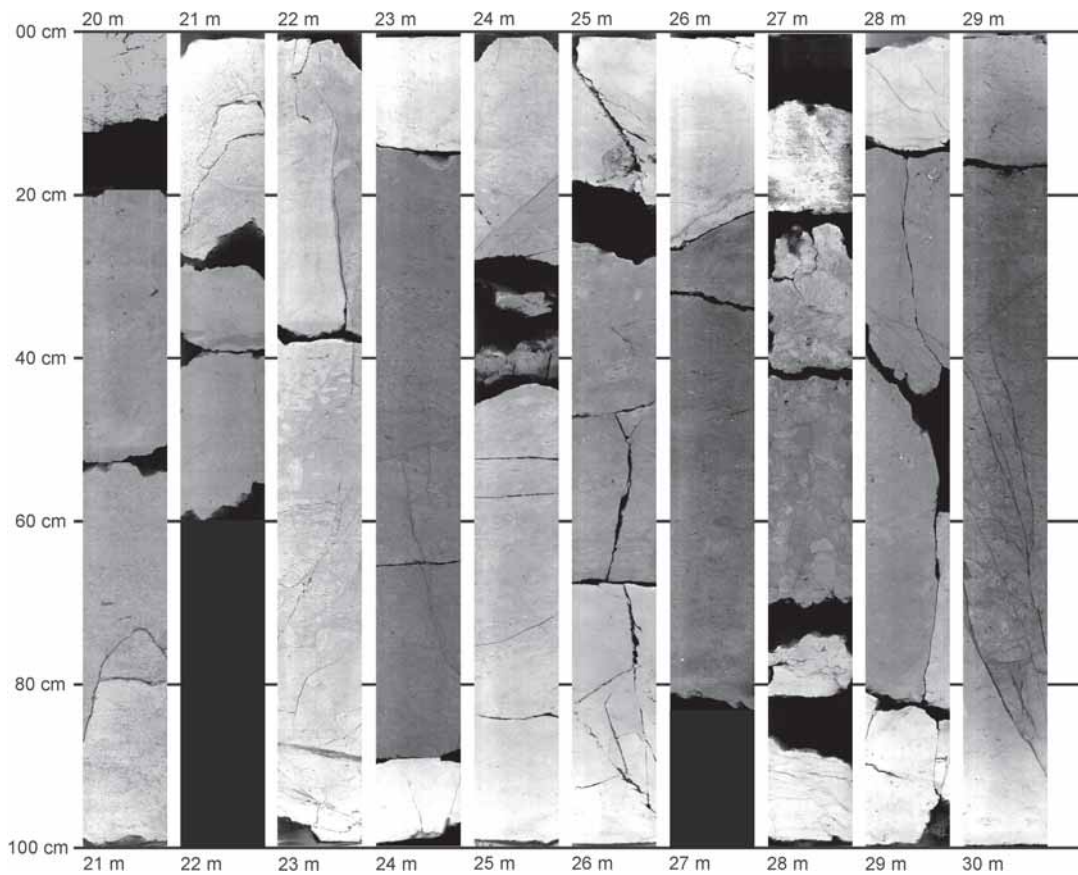
Basin — a study in basin evolution. *Bull. Amer. Assoc. Petrol. Geol. Mem. 45*, 333–346.

Wessely G., Ćorić S., Rögl F., Draxler I. & Zorn I. 2007: Geologie und Paläontologie von Bad Vöslau (Niederösterreich). *Jb. Geol. Bundesanst. 147*, 419–448.

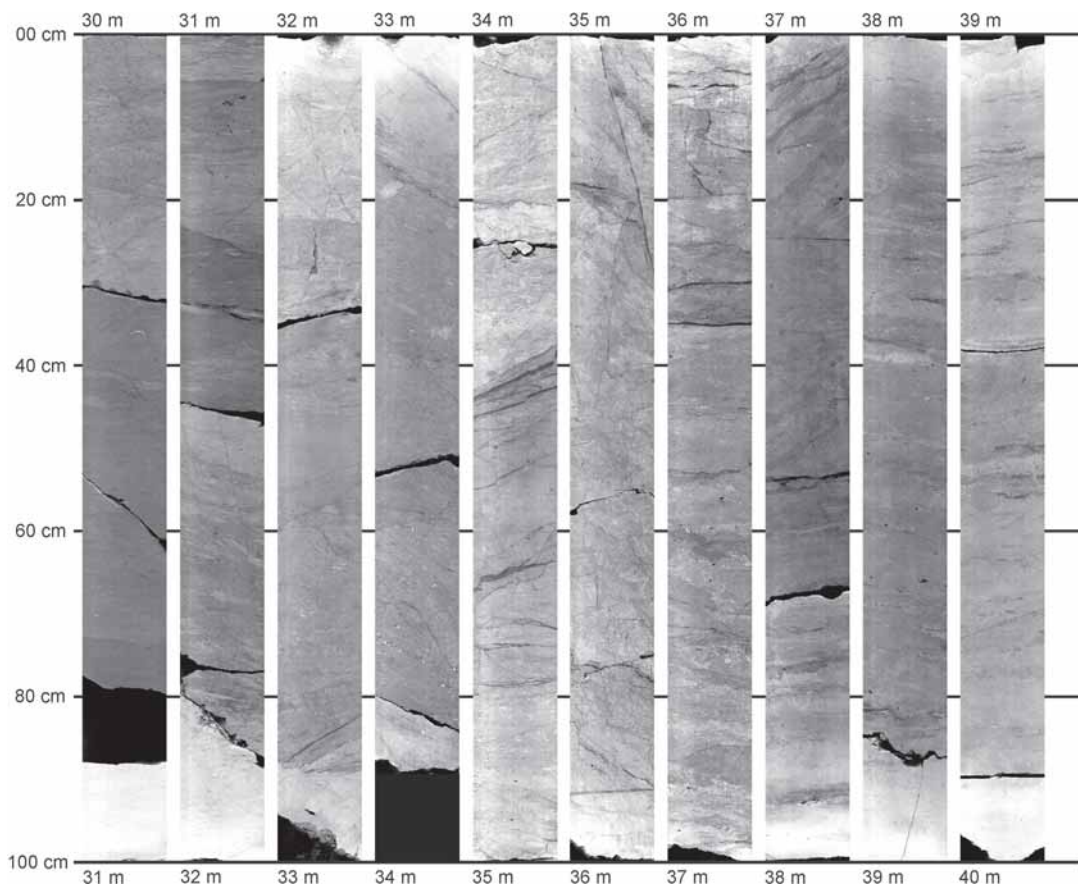
Appendix 1



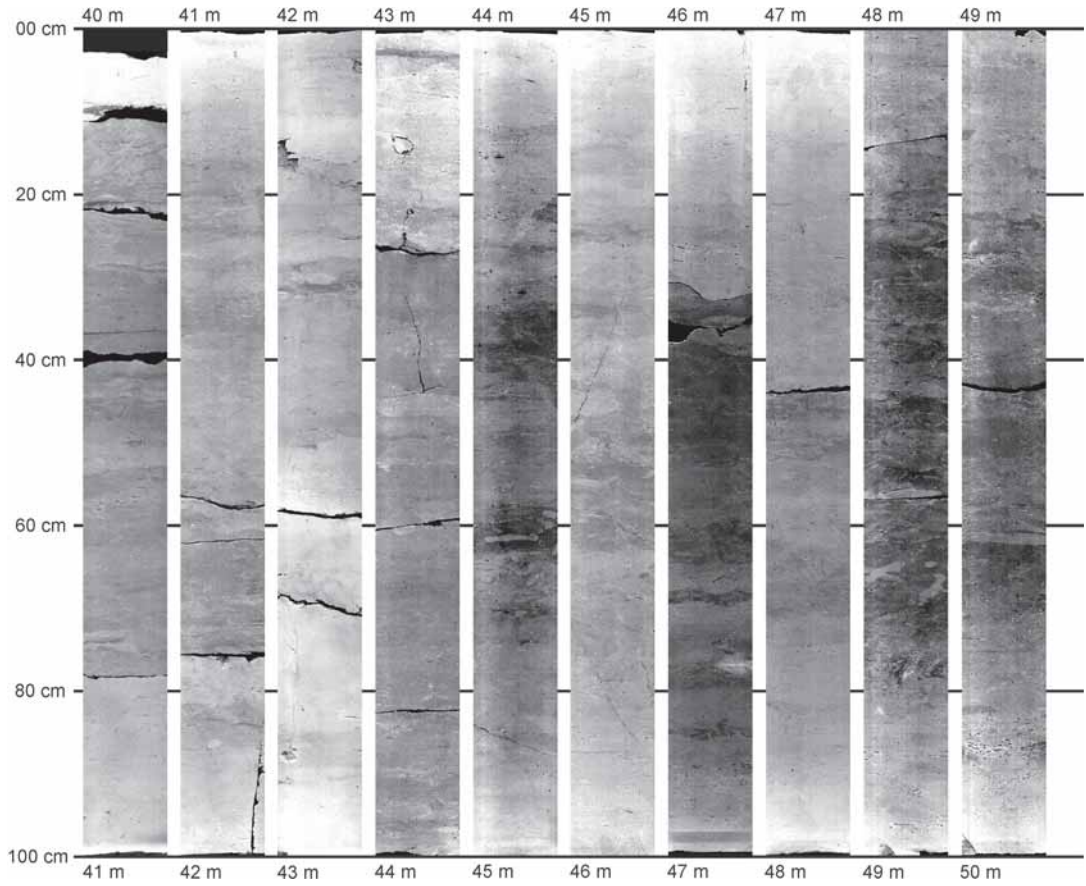
A. Log meters 8 to 20.



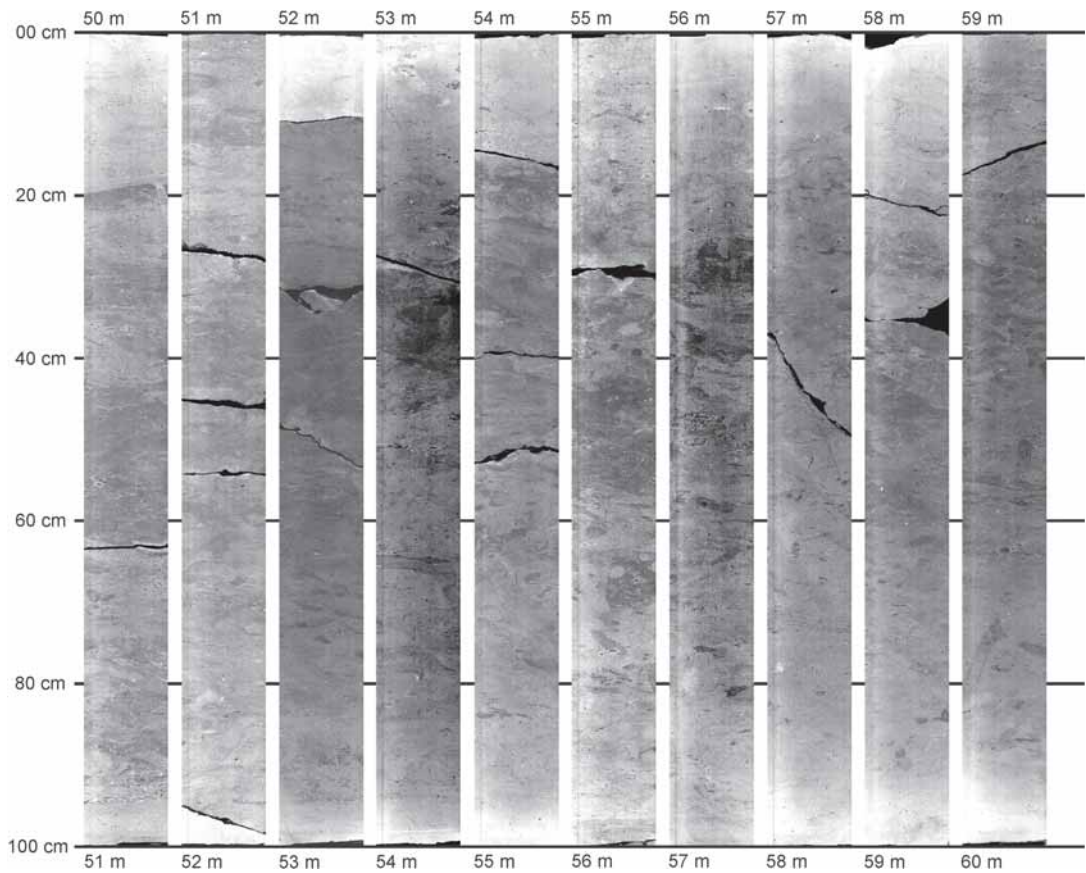
B. Log meters 20 to 30.



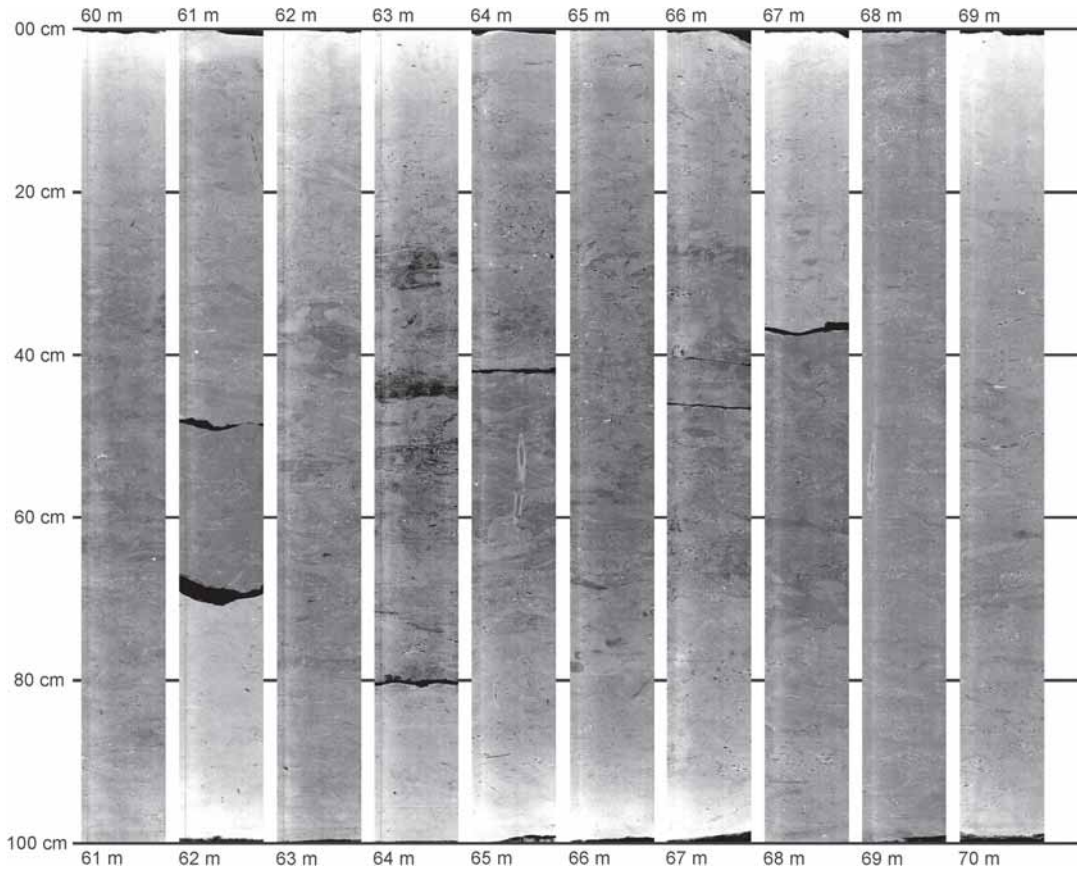
C. Log meters 30 to 40.



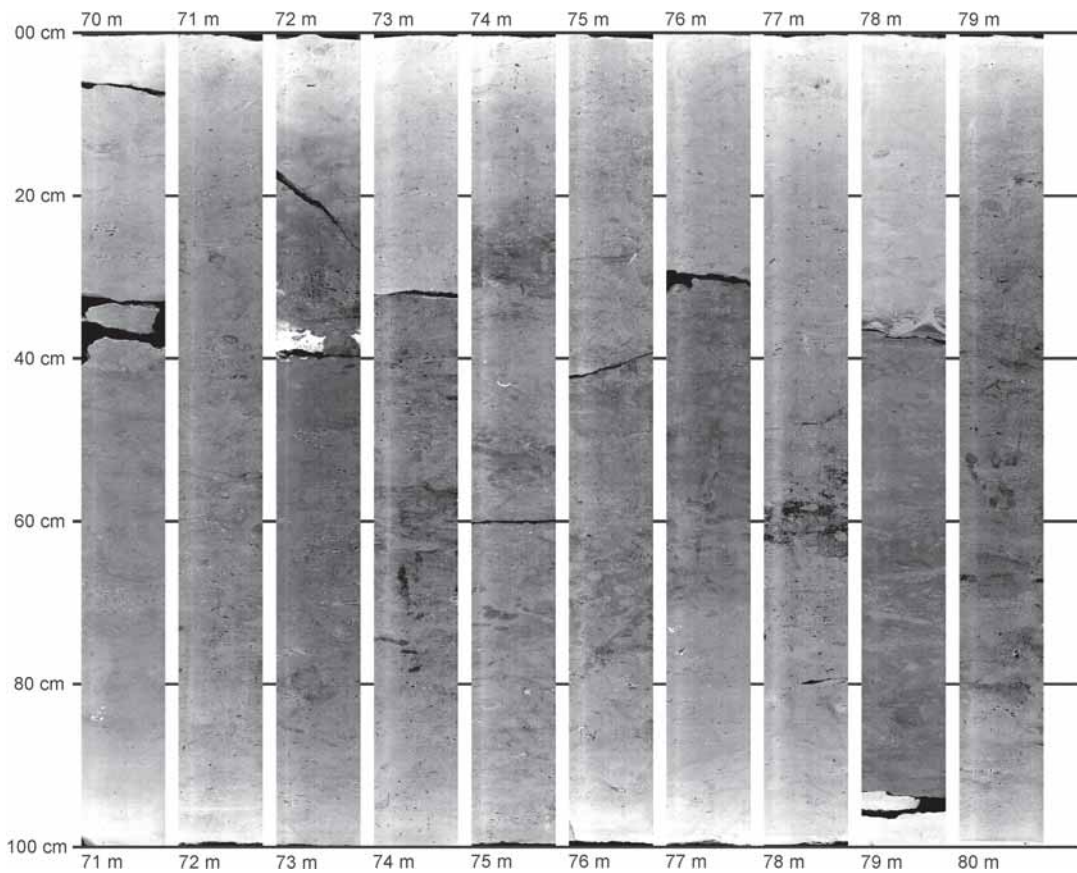
D. Log meters 40 to 50.



E. Log meters 50 to 60.



F. Log meters 60 to 70.



G. Log meters 70 to 80.

